University of Groningen

Faculty of Mathematics & Natural Sciences: Physics

Master Thesis

The Quantum State of a Black Hole

Perturbations to the Hartle-Hawking state

Author:
Rik van Breukelen

First supervisor:
Dr. Kyriakos Papadodimas
Second supervisor:
Dr. Diederik Roest

August 23, 2014

Abstract

We use the thermofield doubling to study black holes. The quantum state of a black hole is obtained from the near horizon approximation for a black hole and from the AdS/CFT correspondence for the BTZ black hole. We perturb this state by changing the phases. This causes no effects outside the black hole, while the geometry of the inside of the black hole is changed.

Contents

1 Introduction

Black hole solutions to the Einstein equations have been of much interest ever since they were first found by Schwarzschild. First disputed as non-physical objects, they are now widely accepted as physical objects. However, to this day, black holes are not fully understood. A black hole is an object where gravity, relativity and quantum mechanics are all important. Moreover, some of these three fundamentals of modern physics seem to contradict each other in black holes. Where quantum mechanics demand unitarity, general relativity does not allow information to escape a black hole. This is called the information paradox [1].

The information paradox persists even after taking Hawking radiation into account. The linearity of quantum mechanics forbids doubling of information, therefore the information cannot be both inside and outside the black hole. This paradox is still not solved. An idea to solve this, is that a firewall at the event horizon destroys the in falling information [2, 3]. However, this would make the event horizon a special place, which contradicts the equivalence principle [3].

To better understand black holes, we look at the quantum state of a black hole, and how perturbations to that state affect the space-time geometry.

We consider the quantum state of a black hole for a free scalar field. This is the Hartle-Hawking state. We construct the inside of the black hole through analytic continuation and find a smooth transition across the horizon. To further study the black hole, we perturb the Hartle-Hawking state and see how the perturbation to that quantum state affects the space-time geometry of the black hole.

In section 2, we look at Rindler space: both as a toy-model for a black hole and as an approximation to the near horizon patch of space. We derive the Unruh effect and obtain the temperature of a black hole. We also derive the Hartle-Hawking state for this system.

We perturb this Hartle-Hawking state in section 3. We perturb the state in such a way that the outside of a black hole is unaffected, however, we see that the geometry of the black hole is changed.

As an explicit example of a black hole, we study the BTZ black hole in section 4. The BTZ black hole is studied with the AdS/CFT correspondence together with Maldacena's proposal that a black hole is dual to two CFTs [4]. Similar to the Rindler case, we construct the inside of the black hole through analytic continuation and obtain the Hartle-Hawking state. We look how perturbations to that state affect the geometry of the space.

In section 5, we check whether the results of the previous sections would be applicable to other black holes. We compare their internal modes to those of the Rindler and BTZ cases.

We will use $-+++$ as our convention for the signature of the metric. Furthermore we use $\hbar = c = G = k_B = 1$ to define our units.

2 Rindler space

Rindler space-time is equivalent to the normal Minkowski space-time, thus we already know what to expect as we are all familiar with Minkowski space. We will use Rindler space as a toy model as Rindler space-time also resembles the space near a black hole horizon. A review of quantum fields in curved space can be found in [5].

2.1 Rindler coordinates

Rindler coordinates describe the same space as Minkowski coordinates, however, where in Minkowski space-time a observer has uniform proper acceleration, the observer is stationary in Rindler space-time. Curves with uniform proper acceleration are hyperbolic curves, therefore we can relate Minkowski coordinates and Rindler coordinates as follows:

$$x = \rho \cosh(\tau) \tag{1}$$

$$t = \rho \sinh(\tau) \tag{2}$$

Where x and t are the normal Minkowski coordinates and ρ and τ are the Rindler coordinates. This describes the patch of Minkowski space shown in figure 1.

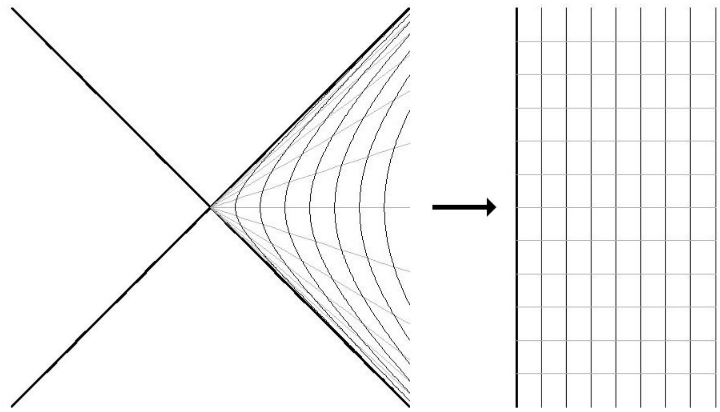

Figure 1: Left Minkowski space, right Rindler space. In both cases the thin black curves are constant ρ curves, the grey curves are constant τ curves.

Therefore we need four sets of Rindler coordinates to fully cover the entire Minkowski space-time. Each wedge will have independent coordinates, furthermore we will label each wedge with either R (right), L (left), P (past) or F (future) where it is necessary to distinguish between the wedges. In figure 2 this labelling is shown. So we have four sets of coordinates:

$$R \qquad x = \rho \cosh(\tau) \tag{3}$$
$$t = \rho \sinh(\tau) \tag{4}$$

$$L \qquad x = -\rho \cosh(\tau) \tag{5}$$
$$t = -\rho \sinh(\tau) \tag{6}$$

$$P \qquad x = -\rho \sinh(\tau) \tag{7}$$
$$t = -\rho \cosh(\tau) \tag{8}$$

$$F \qquad x = \rho \sinh(\tau) \tag{9}$$
$$t = \rho \cosh(\tau) \tag{10}$$

With these coordinates the metric of Rindler space can be obtained. Starting from the metric of Minkowski space

$$ds^2 = -dt^2 + dx^2 \tag{11}$$

we obtain

$$R, L \qquad ds^2 = -\rho^2 d\tau^2 + d\rho^2 \tag{12}$$
$$P, F \qquad ds^2 = \rho^2 d\tau^2 - d\rho^2 \tag{13}$$

From the metric it is clear that shifts in τ leave the metric invariant. These shift correspond with hyperbolic boosts in Minkowski space, the Lorentz boosts. Although these four coordinate sets are independent, if we want to use them together to cover Minkowski space we need make a choice for the direction for the flow of time to obtain smooth transitions at the boundaries of each wedge. The natural choice to follow the time-like Killing field (these choices for the signs of τ are already included in equations (3) to (10)), as depicted in figure 2.

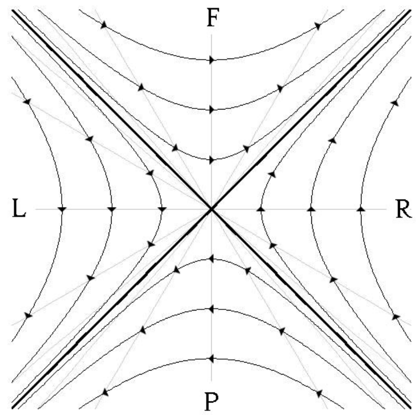

Figure 2: Four Rindler wedges together cover the entire Minkowski space. The arrows follow the time-like Killing Field.

So far we have discussed only $1+1$ dimensional space. We are free to include more dimensions, however, these extra dimensions will remain unchanged. For example $3+1$ Rindler space metric in the right wedge is (depending on the type of coordinate system):

$$ds^2 = -\rho^2 d\tau^2 + d\rho^2 + dy^2 + dz^2 \tag{14}$$

Often we are only interested in the dimensions that for the Rindler space and forgo discussion of the other orthogonal dimensions.

2.2 Rindler space and black holes

Rindler space geometry is closely related to black hole geometry. If a Rindler observer in wedge R is careless and passes to wedge F he would need accelerate beyond the speed of light to return to wedge R. Therefore the boundary between two Rindler wedges is similar to the event horizon of a black hole. Moreover a free falling observer in wedge R will fall towards the horizon, however, just like with a black hole it will take an infinite amount of (Rindler) time to reach the horizon, as shown in figure 3.

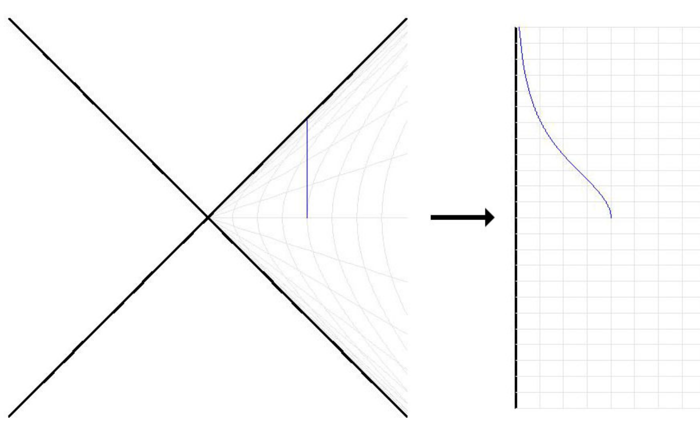

Figure 3: Left Minkowski space, right Rindler space. The blue line is particle at rest falling to the horizon.

We know that a free falling particle in Rindler space will follow a straight line in Minkowski space. So in

Rindler coordinates

$$\rho = \sqrt{x^2 - y^2} \tag{15}$$
$$\tau = \operatorname{arctanh}(y/x) \tag{16}$$

as we aproach the boundary we have:

$$\text{as } t \uparrow x \tag{17}$$
$$\rho \to 0 \tag{18}$$
$$\tau \to \infty \tag{19}$$

Rindler coordinates are a useful tool in the study of black holes. For example the metric of the Schwarzschild black hole can be written as the Rindler metric when we look close to the horizon. The Schwarzschild metric is

$$ds^2 = -\left(1 - \frac{r_0}{r}\right) dt^2 + \left(1 - \frac{r_0}{r}\right)^{-1} dr^2 + r^2 d\Omega^2 \tag{20}$$
$$d\Omega^2 = d\theta^2 + \sin(\theta)^2 d\phi^2 \tag{21}$$

where $r_0 = 2M$. in the near horizon expansion we have $r - r_o = \varepsilon$ and ignore higher orders of ε. The metric then reduces to

$$ds^2 = -\frac{\varepsilon}{r_0} dt^2 + \frac{r_0}{\varepsilon} d\varepsilon^2 + r_0^2 d\Omega^2 \tag{22}$$

setting $4r_0\varepsilon = \rho^2$ and $t = \frac{1}{2r_0}\tau$ we obtain:

$$ds^2 = -\rho^2 d\tau^2 + d\rho^2 + r_0^2 d\Omega^2 \tag{23}$$

which is just the Rindler metric together with the metric of a sphere with radius r_0. Therefore close to the horizon we obtain Rindler space. Furthermore because we know that we can rewrite these coordinates again as a patch of Minkowski space we conclude that at a classical level we expect no strange behaviour at the horizon.
Rindler space can also be used to calculate the temperature of a black hole in quick manner. We Wick rotate to Euclidean space $\tau = -i\tau_E$ and obtain the metric of Euclidean space in polar coordinates.

$$ds^2 = \rho^2 d\tau_E^2 + d\rho^2 \tag{24}$$

To avoid conical singularities we need to identify $\tau_E = \tau_E + 2\pi$, and as shown in appendix A.1 we conclude that the system is at $T = \frac{1}{2\pi}$. Furthermore in the case of the Schwarzschild metric we scaled the time with $t = \frac{1}{2r_0}\tau$ to obtain the Rindler metric, therefore the imaginary time t_E should be periodic with period $\beta = 4r_0\pi$ to avoid conical singularities. Thus the temperature of a Schwarzschild black hole is $T = \frac{1}{8M\pi} = \frac{\hbar c^3}{8M\pi G k_B}$. For the Rindler temperature we will provide a more rigorous proof in section 2.6.

2.3 Wave modes

To study the effects of a black hole horizon we place a scalar field with mass m on the background of the Rindler metric. A scalar field obeys the Klein-Gordon equation.

$$\Box\psi = m^2\psi \tag{25}$$

In a curved background this becomes [5]:

$$\frac{1}{\sqrt{-g}} \partial_\mu \sqrt{-g} g^{\mu\nu} \partial_\nu \psi = m^2 \psi \tag{26}$$

Using the ansatz $\psi(\tau, \rho) = e^{-i\omega\tau} f_\omega(\rho)$ together with the Rindler metric in the R wedge, we obtain:

$$\rho^2 f''_\omega + \rho f'_\omega - (\rho^2 m^2 - \omega^2) f_\omega = 0 \tag{27}$$

Therefore our solution is of the form:

$$f_\omega(\rho) = N_\omega K_{i\omega}(m\rho) \tag{28}$$

where N_ω is some normalization constant and $K_\alpha(x)$ is the modified Bessel function of the second kind. Although the equation is also solved by the modified Bessel function of the first kind, that solution rejected because it has infinite energy. We decompose the field in positive and negative frequency waves. Thus our field operator in the right wedge is:

$$\Psi_R(\tau,\rho) = \int_{\omega>0} \frac{d\omega}{2\pi}\frac{1}{\sqrt{2\omega}}\left(a_{R,\omega}\psi_{R,\omega}(\tau,\rho) + \text{h.c.}\right) \tag{29}$$

$$\psi_{R,\omega}(\tau,\rho) = e^{-i\omega\tau} N_\omega K_{i\omega}(m\rho) \tag{30}$$

A similar expression holds for the left wedge, however, as the time runs backward we should choose a different sign for ω.

$$\psi_{L,\omega}(\tau,\rho) = e^{i\omega\tau} N_\omega K_{-i\omega}(m\rho) \tag{31}$$

So at this point we can describe the fields in the left and right wedges.

2.4 Behind the horizon

Behind the horizon of a black hole corresponds to the future wedge of the Rindler space-time. We repeat the discussion of last subsection for the future wedge (the past wedge is similar to the future wedge). The main difference between the future and the right wedge is the sign in the metric (12), (13). Which effectively flips the sign of m^2 in equation (27).

$$\rho^2 f''_\omega + \rho f'_\omega + (\rho^2 m^2 + \omega^2) f_\omega = 0 \tag{32}$$

therefore our solution is of the form:

$$\psi_{F,\omega}(\tau,\rho) = e^{-i\omega\tau}\hat{N}_\omega J_{i\omega}(m\rho) \tag{33}$$

where $\hat{N}_\omega$ is some normalization constant and $J_\alpha(x)$ is the Bessel function of the first kind. Because τ is now a space-like direction, we no long decompose this into positive and negative frequency waves. We have to consider the entire frequency range, however, for calculation it is more convenient to write them separately. Moreover, Bessel functions of the first kind can be written as a linear combination of modified Bessel functions of the second kind, which makes it easier to compare with the modes in the right wedge. Therefore our modes in the future wedge are.

$$\psi_{1,\omega}(\tau,\rho) = e^{-i\omega\tau}\tilde{N}_\omega K_{i\omega}(-im\rho) \tag{34}$$

$$\psi_{2,\omega}(\tau,\rho) = e^{i\omega\tau}\tilde{N}_\omega K_{-i\omega}(-im\rho) \tag{35}$$

where in the second mode we have flipped the sign of ω to obtain only positive ω for the field operator:

$$\Psi_F(\tau,\rho) = \int_{\omega>0} \frac{d\omega}{2\pi}\frac{1}{\sqrt{2\omega}}\left(a_{1,\omega}\psi_{1,\omega}(\tau,\rho) + a_{2,\omega}\psi_{2,\omega}(\tau,\rho) + \text{h.c.}\right) \tag{36}$$

which describes the fields in the future wedge.
We now have two sets of annihilation and creation operators, the left and right one and the operators from the future wedge, while only one is needed to hold all the information. Therefore the right field (29) and its left partner describe the same information as the future field (36). Therefore we are able to link the creation and annihilation operators of the left and right wedges to the future wedge.
We analytically continue the modes of the right wedge to the future wedge. This is most easily done using light-cone coordinates.

$$u = t + x \tag{37}$$

$$v = t - x \tag{38}$$

$$\rho = \sqrt{-uv} \tag{39}$$

$$\tau = \frac{1}{2}\ln(u) - \frac{1}{2}\ln(-v) \tag{40}$$

The expressions for ρ and τ hold for the right wedge and changes for the other wedges. The R mode and the future modes in the future wedge look like:

$$\psi_{R,\omega}(u,v) = e^{-i\omega\frac{1}{2}(\ln u - \ln v)} N_\omega K_{i\omega}(im\sqrt{uv}) \tag{41}$$

$$\psi_{1,\omega}(u,v) = e^{-i\omega\frac{1}{2}(\ln u - \ln v)} \tilde{N}_\omega K_{i\omega}(-im\sqrt{uv}) \tag{42}$$

$$\psi_{2,\omega}(u,v) = e^{i\omega\frac{1}{2}(\ln u - \ln v)} \tilde{N}_\omega K_{-i\omega}(-im\sqrt{uv}) \tag{43}$$

So in fact $\psi_{R,\omega}(u,v) \sim \psi^\dagger_{2,\omega}(u,v)$, furthermore we repeat the same for the left wedge and obtain $\psi_{L,\omega}(u,v) \sim \psi^\dagger_{1,\omega}(u,v)$. Therefore we can relate the creation and annihilation operators in the left and right wedges to the future wedge operators.

$$a_{R,\omega} = a^\dagger_{2,\omega} \tag{44}$$

$$a^\dagger_{R,\omega} = a_{2,\omega} \tag{45}$$

$$a_{L,\omega} = a^\dagger_{1,\omega} \tag{46}$$

$$a^\dagger_{L,\omega} = a_{1,\omega} \tag{47}$$

Intuitively speaking this exchange between creation and annihilation operators is to be expected. A particle passing the boundary between the right wedge and the future wedge is destroyed in the right wedge and created in the future wedge. Using this prescription we have found a smooth way to relate all the wedges.

2.5 Minkowski modes

The left and right wedges contained the same information as the future wedge and could be connected to each other. However, as we seen in section 2.1 the Rindler coordinates describe the same space as Minkowski coordinates. Therefore we can relate the Rindler modes to the Minkowski modes. As the future modes are related to the left and right modes we only have to relate the Minkowski modes to one set of modes. We will rewrite the left and right modes as follows:

$$\psi^{\text{Rin}}_{R,\omega} = \begin{cases} \psi_{R,\omega} & \text{In region } R \\ 0 & \text{In region } L \end{cases} \tag{48}$$

$$\psi^{\text{Rin}}_{L,\omega} = \begin{cases} 0 & \text{In region } R \\ \psi_{L,\omega} & \text{In region } L \end{cases} \tag{49}$$

Furthermore with constant ρ we can rewrite $\tau = -\ln(\rho) + \ln(u)$ in the R region. So the above equation become:

$$\psi^{\text{Rin}}_{R,\omega} \sim \begin{cases} e^{-i\omega\tau} \sim e^{-i\omega\ln(u)} & \text{In region } R \\ 0 & \text{In region } L \end{cases} \tag{50}$$

$$\psi^{\text{Rin}}_{L,\omega} \sim \begin{cases} 0 & \text{In region } R \\ e^{i\omega\tau} \sim e^{i\omega\ln(-u)} & \text{In region } L \end{cases} \tag{51}$$

Let $\psi^{\text{Min}}_{1,\omega}$ be the Minkowski modes corresponding to the positive frequency solution. These Minkowski modes will have contributions of all Rindler modes with forward moving modes, forward from the point of view if Minkowski observer. These are the $\psi^{\text{Rin}}_{R,\omega}$ and $\psi^{\text{Rin}\,\dagger}_{L,\omega}$ modes. Therefore the Minkowski modes will be of the form:

$$\psi^{\text{Min}}_{1,\omega} = N \begin{cases} a\psi_{R,\omega} & \text{In region } R \\ b\psi^\dagger_{L,\omega} & \text{In region } L \end{cases} \tag{52}$$

where a, b are some constants and N is a normalization factor. Furthermore we require analyticity around $u = 0$. When analytically continue the R modes into the L region (where u is negative) we obtain:

$$\psi^{\text{Rin}}_{R,\omega} \sim e^{-i\omega \ln(u)} = e^{-i\omega \ln((-1)(-u))} = e^{-i\omega \ln(-u)} e^{-\omega\pi} \sim e^{-\pi\omega} \psi^{\text{Rin}\,\dagger}_{L,\omega} \tag{53}$$

So our positive frequency Minkowski modes become:

$$\psi^{\text{Min}}_{1,\omega} = \left(\psi^{\text{Rin}}_{R,\omega} + e^{-\pi\omega} \psi^{\text{Rin}\,\dagger}_{L,\omega}\right) / (1 - e^{-2\pi\omega})^{\frac{1}{2}} \tag{54}$$

Similarly the negative frequency Minkowskki modes are:

$$\psi^{\text{Min}}_{2,\omega} = \left(\psi^{\text{Rin}}_{L,\omega} + e^{-\pi\omega} \psi^{\text{Rin}\,\dagger}_{R,\omega}\right) / (1 - e^{-2\pi\omega})^{\frac{1}{2}} \tag{55}$$

Using these relations we can relate the creation and annihilation operators of the left and right wedges to the creation and annihilation operators of the positive and negative frequency modes, which will denote with $b_1, b_1^\dagger, b_2, b_2^\dagger$.

$$b_{1,\omega} = \left(a_{R,\omega} - e^{-\pi\omega} a^\dagger_{L,\omega}\right) / (1 - e^{-2\pi\omega})^{\frac{1}{2}} \tag{56}$$

$$b_{2,\omega} = \left(a_{L,\omega} - e^{-\pi\omega} a^\dagger_{R,\omega}\right) / (1 - e^{-2\pi\omega})^{\frac{1}{2}} \tag{57}$$

$$a_{R,\omega} = \left(b_{1,\omega} + e^{-\pi\omega} b^\dagger_{2,\omega}\right) / (1 - e^{-2\pi\omega})^{\frac{1}{2}} \tag{58}$$

$$a_{L,\omega} = \left(b_{2,\omega} + e^{-\pi\omega} b^\dagger_{1,\omega}\right) / (1 - e^{-2\pi\omega})^{\frac{1}{2}} \tag{59}$$

As these operators are related non-trivially we need to take care on what state we act. For example if we act with an Minkowski annihilation operator on the Rindler vacuum we observe the following.

$$b_{1,\omega} |0, \text{Rin}\rangle = \left(a_{R,\omega} - e^{-\pi\omega} a^\dagger_{L,\omega}\right) / (1 - e^{-2\pi\omega})^{\frac{1}{2}} |0, R\rangle |0, L\rangle \tag{60}$$

$$= -\frac{e^{-\pi\omega}}{(1 - e^{-2\pi\omega})^{\frac{1}{2}}} |0, R\rangle |1, L\rangle \tag{61}$$

Thus what is empty space for a Rindler observer is not empty for a Minkowski observer, and vice versa. This is called the Unruh effect.

It is important to note that the Minkowski modes used are not the Minkowski modes that are usually used. They are labelled with some frequency ω, while usually we label them with momentum k. The relation between these different Minkowski modes is non-trivial, however, they do contain the same information.

2.6 Entangled state as ground state

As shown in the last section the Minkowski vacuum is not equal to the Rindler vacuum. However, as Minkowski space-time and Rindler space-time describe the same space there should be a corresponding Rindler state for the Minkowski vacuum. Therefore the Minkowski vacuum can be rewritten on the basis of Rindler n-particle states.

$$|0, \text{Min}\rangle = \sum_{m,n} c_{m,n} |m, L\rangle |n, R\rangle \tag{62}$$

To remove all non-physical states we set $c_{m,n} = 0$ for all $m < 0$ or $n < 0$. If we act with an Minkowski annihilation operator on this state it should give zero.

$$b_{1,\omega} |0, \text{Min}\rangle = \frac{1}{(1 - e^{-2\pi\omega})^{\frac{1}{2}}} \left(a_{R,\omega} - e^{-\pi\omega} a^\dagger_{L,\omega}\right) \sum_{m,n} c_{m,n} |m, L\rangle |n, R\rangle \tag{63}$$

$$= \frac{1}{(1 - e^{-2\pi\omega})^{\frac{1}{2}}} \sum_{m,n} (-c_{m,n}\sqrt{m+1} e^{-\pi\omega} + c_{m+1,n+1}\sqrt{n+1}) |m+1, L\rangle |n, R\rangle \tag{64}$$

This should be zero for all Rindler states, therefore:

$$c_{m,n}\sqrt{n+1}e^{-\pi\omega} = c_{m+1,n+1}\sqrt{m+1} \tag{65}$$

A similar procedure for $b_{2,\omega}$ gives:

$$c_{m,n}\sqrt{m+1}e^{-\pi\omega} = c_{m+1,n+1}\sqrt{n+1} \tag{66}$$

These two equations together with $c_{m,n} = 0$ for all $m < 0$ or $n < 0$ give that only the diagonal elements are non-zero, or more specific:

$$c_{n,n} = c_{0,0}e^{-n\pi\omega} \tag{67}$$

for positive n. Therefore the normalized Minkowski vacuum is

$$|0, \text{Min}\rangle = \prod_j \left((1 - e^{-2\pi\omega_j})^{\frac{1}{2}} \sum_{n_j=0}^{\infty} e^{-n_j\pi\omega_j} |n_j, L\rangle |n_j, R\rangle \right) \tag{68}$$

For a Rindler observer who can only observe the right wedge this looks like a thermal ensemble. We trace out the left system as the Rindler observer in the right wedge is unable to intact with the left side.

$$\rho_R = \sum_L |0, \text{Min}\rangle \langle 0, \text{Min}| \tag{69}$$

$$= \prod_j \left((1 - e^{-2\pi\omega_j}) \sum_{n_j=0}^{\infty} e^{-2n_j\pi\omega_j} |n_j, R\rangle \langle n_j, R| \right) \tag{70}$$

Which is density matrix corresponding to thermal ensemble of $T = \frac{1}{2\pi}$. Another way to obtain the temperature is to calculate the spectrum of Rindler particles of the Minkowski vacuum.

$$N_{R,\omega} = a^{\dagger}_{R,\omega} a_{R,\omega} \tag{71}$$

$$\langle 0, \text{Min}| N_{R,\omega} |0, \text{Min}\rangle = (1 - e^{-2\pi\omega}) \sum_{n=0}^{\infty} \left(e^{-2\pi\omega}\right)^n \langle n_j, R| \langle n_j, L| N_{R,\omega} |n_j, L\rangle |n_j, R\rangle \tag{72}$$

$$= \frac{1}{e^{2\pi\omega} - 1} \tag{73}$$

Which is the Planck's law corresponding to the black body radiation with a temperature of $T = \frac{1}{2\pi}$. Therefore we can rewrite all physics from the Minkowski space-time into the physics of the Rindler space-time, which closely resembles the behaviour of a black hole. The main difference is that where the Minkowski vacuum corresponds to an empty state for a Minkowski observer it is not empty for a Rindler observer. However, combining the four Rindler wedges, the correspondence between the creation and annihilation between the different wedges and the correspondence between Rindler and Minkowski modes together with the entangled state just discussed, we have obtained a smooth description which is equivalent to the normal Minkowski description.

3 Pertubations to the Hartle-Hawking state

In 1976 Israel proposed that the space-time of a black hole can be described as an entangled state [6].

$$|\Psi\rangle = \frac{1}{\sqrt{Z(\beta)}} \sum_n e^{-\beta E_n/2} |E_n\rangle_1 \times |E_n\rangle_2 \tag{74}$$

This is called the Hartle-Hawking state. Writing a real time thermal field as two entangled systems is used in thermofield dynamics as a mathematical tool. However, for black holes this method might by provide a description that can be used to describe the inside of a black hole.

We have already noted that the Rindler space-time closely resembles that of the space close to the horizon of a black hole, moreover the Rindler state (68) corresponding to the Minkowski vacuum is an entangled states of the form (74). If we drop normalization we have

$$|\Psi\rangle \sim \sum_n e^{-\beta E_n/2} |E_n\rangle_1 \times |E_n\rangle_2 \tag{75}$$

$$|0,\mathrm{Min}\rangle \sim \sum_n e^{-n\pi\omega} |n,L\rangle \times |n,R\rangle \tag{76}$$

Where for the Rindler states we have $\beta = T^{-1} = 2\pi$ and $E_n = n\omega$. For the energy of the Rindler state we have dropped the zero point energy which will be taken care of by the normalization. Then these equations are the same. The Rindler space resembles a black hole even in this regard. If we only have information on the right wedge of Rindler space, or similarly the right outside the black hole patch, we can change the state without it affecting our physics. For example

$$|\Psi\rangle = \frac{1}{\sqrt{Z(\beta)}} \sum_n e^{i\delta(n,\omega)} e^{-\beta E_n/2} |E_n\rangle_1 \times |E_n\rangle_2 \tag{77}$$

where $\delta(n,\omega)$ is some real function of n and ω. This state has the same physics outside the black hole. It has the same entanglement entropy, the same temperature. Requiring that all these phases are zero is fine tuning of an infinite number of parameters. We will discuss the effect of such a random phase in the next sections.

3.1 Simple phase changes

First we will discuss a group of phase changes with a clear interpretation. As stated in section 2.1 the direction of the flow of time as we have defined follows a Killing field. Therefore time evolution using the following Hamiltonian will leave the system invariant.

$$H = H_R - H_L \tag{78}$$

Where H_R and H_L are the Hamiltonians of the right and left wedge respectively. This corresponds to the time flowing 'up' in the right wedge and 'down' in the right wedge, as depicted in figure 2. If we let the time flow 'up' in both wedges the system will not be invariant under time evolution of the corresponding Hamiltonian.

$$\tilde{H} = H_R + H_L \tag{79}$$

Which changes the state as follows (looking only at a single frequency):

$$e^{-i(H_R+H_L)t} |0,\mathrm{Min}\rangle = (1-e^{-2\pi\omega})^{\frac{1}{2}} \sum_{n=0}^{\infty} e^{-n_j\pi\omega} e^{-2i\omega n t} |n,L\rangle |n,R\rangle \tag{80}$$

up to a overall frequency factor.
This time shift acted on both the left and right wedges, however, we can obtain the same phases by only acting on the left wedge. We can combine the 'Killing' time evolution with the 'up' time evolution If we do this with the same magnitude but with opposing sign then the right remain unchanged.

$$e^{-iHt} e^{-i\tilde{H}(-t)} = e^{-2iH_L t} \tag{81}$$

Therefore this phase change goes unnoticed when restricted to the right wedge, only when both the information of the left and right wedges is used is this phase change noticed. For example when we look at effect of a phase change corresponding to a upward time shift with magnitude t_p. The state is

$$|\widetilde{0,\mathrm{Min},t_p}\rangle = (1-e^{-2\pi\omega})^{\frac{1}{2}} \sum_{n=0}^{\infty} e^{-n_j\pi\omega} e^{-2i\omega n t_p} |n,L\rangle |n,R\rangle \tag{82}$$

Which changes the two-point function of the creation and annihilation opperators as follows:

$$\langle 0, \widetilde{\text{Min}, t_p} | a_{R,\omega} a_{L,\omega'} | 0, \widetilde{\text{Min}, t_p} \rangle = e^{-2i\omega t_p} \frac{1}{e^{\pi\omega} - e^{-\pi\omega}} \delta(\omega - \omega') \tag{83}$$

The other two point functions can either be obtained by taking the Hermitian of this one, or they remain unchanged. With this two-point function we can calculate the two-point function of the scalar field.

$$\langle 0, \widetilde{\text{Min}, t_p} | \Psi_R(0,\rho) \Psi_L(0,\rho) | 0, \widetilde{\text{Min}, t_p} \rangle = \int_{\omega>0} \frac{d\omega}{(2\pi)^2} \frac{1}{\omega} N_\omega^2 K_{i\omega}(m\rho) K_{-i\omega}(m\rho) \frac{cos(2\omega t_p)}{e^{\pi\omega} - e^{-\pi\omega}} \tag{84}$$

Which according to appendix A.2 should be related to the geodesic distance like:

$$\langle 0, \widetilde{\text{Min}, t_p} | \Psi_R(0,\rho) \Psi_L(0,\rho) | 0, \widetilde{\text{Min}, t_p} \rangle \sim e^{-md} \tag{85}$$

where d is geodesic distance between the two points. The geodesic distance is non-trivial to calculate in Rindler space, however, in Minkowski space it is trivial.

$$d(x,t) = \sqrt{|dx^2 - dt^2|} \tag{86}$$

Which for the above situation is:

$$d = 2\rho \tag{87}$$

It is clear that while (84) decreases with t_p and according to equation (85) the geometric distance should increase, the geometric distance remains unchanged.

We have assumed that geometry of the space did not change by introducing phase changes to the Hartle-Hawking state, and therefore used equation (86) to calculate the geometric distance. However, the phase change did change the geometry. We can undo the phases by letting the upward time evolution act on the operators instead of the state. The two-point function will remain unchanged, however, the two point are at different locations now. Therefore the geometric distance is:

$$d = 2\rho \cosh(t_p) \tag{88}$$

Which does increase with t_p. The addition of the phases to the ground stated changed the geometry of the space. However, as we can produce these phase changes with either an upward time evolution (80) or a one-sided time evolution (81) the geometry within the right or left wedge does not change. The geometry changes at the boundary.

Furthermore because we can produce the phases with the upward and one sided time evolution we can also undo the phases with these operations. Given a Hartle-Hawking state with phases we can redefine our coordinates, shifted in some way, and return to the 'clean' ground state.

While for the left and right wedges these time evolutions are intuitive this is not true for the future (and past) wedge. The field operator in the future wedge (36) can be split into two operators:

$$\Psi_F(\tau,\rho) = \int_{\omega>0} \frac{d\omega}{2\pi} \frac{1}{\sqrt{2\omega}} \left(a_{1,\omega} \psi_{1,\omega}(\tau,\rho) + a_{2,\omega} \psi_{2,\omega}(\tau,\rho) + \text{h.c.} \right) \tag{89}$$

$$= \int_{\omega>0} \frac{d\omega}{2\pi} \frac{1}{\sqrt{2\omega}} \left(a_{1,\omega} \psi_{1,\omega}(\tau,\rho) + \text{h.c.} \right) + \int_{\omega>0} \frac{d\omega}{2\pi} \frac{1}{\sqrt{2\omega}} \left(a_{2,\omega} \psi_{2,\omega}(\tau,\rho) + \text{h.c.} \right) \tag{90}$$

$$= \Psi_1(\tau,\rho) + \Psi_2(\tau,\rho) \tag{91}$$

Where $\Psi_2(\tau,\rho)$ is related to the R wedge and $\Psi_1(\tau,\rho)$ is related to the L wedge, as discussed in section 2.4. Therefore these parts are shifted differently.

While the geometry of the left and right wedges did not change by adding the phases, the geometry of the future wedge is changed. this is most easily seen from the two-point function in the future wedge:

$$\langle 0, \widetilde{\text{Min}, t_p} | \Psi_F(\tau,\rho) \Psi_F(\tau',\rho) | 0, \widetilde{\text{Min}, t_p} \rangle = \langle 0, \widetilde{\text{Min}, t_p} | \big(\Psi_1(\tau,\rho) + \Psi_2(\tau,\rho)\big)\big(\Psi_1(\tau',\rho) + \Psi_2(\tau',\rho)\big) | 0, \widetilde{\text{Min}, t_p} \rangle \tag{92}$$

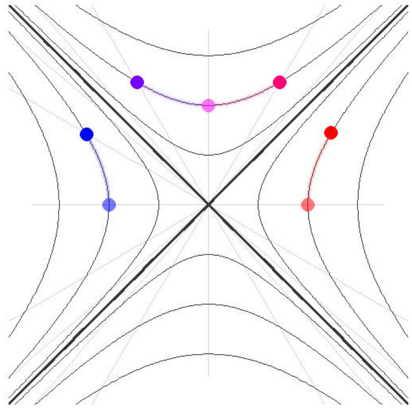

Figure 4: An upward time shift on both wedges splits the future operator into two operators.

$$= \langle 0, \widetilde{\text{Min}, t_p} | \Psi_1(\tau, \rho)\Psi_1(\tau', \rho) | 0, \widetilde{\text{Min}, t_p} \rangle$$
$$+ \langle 0, \widetilde{\text{Min}, t_p} | \Psi_2(\tau, \rho)\Psi_2(\tau', \rho) | 0, \widetilde{\text{Min}, t_p} \rangle$$
$$+ 2 \int_{\omega > 0} \frac{d\omega}{(2\pi)^2} \frac{1}{\omega} N_\omega^2 K_{i\omega}(m\rho) K_{-i\omega}(m\rho) \frac{cos(2\omega t_p + (\tau + \tau')\omega)}{e^{\pi\omega} - e^{-\pi\omega}} \tag{93}$$

The two-point functions of only Ψ_1 or Ψ_2 are independent of the phases, just like the pure left or right two-point functions. On the contrary the cross terms are dependant on the phase change. Therefore the geometry is changed within the future wedge. Furthermore if t_p becomes very large, compared to τ and τ', the left and right wedge disconnect. Both the distance between the two wedges increases and cross terms in two-point functions tend to zero. We can also chose points that come closer together by the changed phases, however for the more general phase changes these points are a minority. As can be seen in the next section.

3.2 General phase changes

In the last section we discussed a simple phase change, now we will construct a general phase change. We act with the following operator on the Hartle-Hawking state.

$$U = e^{-i\omega\theta(\omega)N_L} \tag{94}$$

where N_L is the left wedge number operator. Furthermore $\theta(\omega)$ is a real function of ω. Because different frequencies do not interact there are little constraints on $\theta(\omega)$. It needs to be defined for all $\omega > 0$ and non-singular in that region. It may be discontinuous at every point. The phase changes corresponding to this operator are:

$$U |0, \text{Min}\rangle = (1 - e^{-2\pi\omega})^{\frac{1}{2}} \sum_{n=0}^{\infty} e^{-n\pi\omega} e^{-i\omega n\theta(\omega)} |n, L\rangle |n, R\rangle \tag{95}$$

At the same time the effect of this operator on the left field operator is,

$$U^{-1}\Psi_L(\tau, \rho)U = \int_{\omega > 0} \frac{d\omega}{2\pi} \frac{1}{\sqrt{2\omega}} \left(a_{L,\omega} e^{i\omega(\tau - \theta(\omega))} N_\omega K_{-i\omega}(m\rho) + \text{h.c.} \right) \tag{96}$$

Which is a frequency dependant time shift. Furthermore two-point functions within the left wedge are unaffected by this phase change. However, cross terms between wedges are affected.

$$\langle 0, \widetilde{\text{Min}, \theta(\omega)} | \Psi_R(0, \rho)\Psi_L(0, \rho) | 0, \widetilde{\text{Min}, \theta(\omega)} \rangle = \int_{\omega > 0} \frac{d\omega}{(2\pi)^2} \frac{1}{\omega} N_\omega^2 K_{i\omega}(m\rho) K_{-i\omega}(m\rho) \frac{cos(\omega\theta(\omega))}{e^{\pi\omega} - e^{-\pi\omega}} \tag{97}$$

Which again decreases the two-point function, except for the cases $\theta(\omega) = 0$ and $\theta(\omega) = \frac{c}{\omega}$ with c a real constant. In these cases U is the identity operator or an overall phase change respectively. The previous section dealt with the specific case that $\theta(\omega) = t_p$, however, the conclusions are the same for this more general case: the two-point function decreases and position is shifted if the phases are absorbed into the field operator. The operator is smeared by a frequency dependant time shift.
We can generalise our phases even further. For example, we can look at the following operator.

$$U = e^{-i\omega N_L^2 t_2} \tag{98}$$

Which induces the following phase changes:

$$U|0,\text{Min}\rangle = (1-e^{-2\pi\omega})^{\frac{1}{2}} \sum_{n=0}^{\infty} e^{-n\pi\omega} e^{-i\omega n^2 t_2} |n,L\rangle |n,R\rangle \tag{99}$$

Or effects the field operator as follows, see appendix A.3:

$$U^{-1}\Psi_L(\tau,\rho)U = \int_{\omega>0} \frac{d\omega}{2\pi} \frac{1}{\sqrt{2\omega}} \left(a_{L,\omega} e^{i\omega(\tau+(2N_L-1)t_2)} N_\omega K_{-i\omega}(m\rho) + \text{h.c.} \right) \tag{100}$$

A number operator remains within the field operator. Also in this case the two-point functions within the left or right wedge remain unchanged. And again the cross terms between them are changed.

$$\langle \widetilde{0,\text{Min},t_2} | \Psi_R(0,\rho)\Psi_L(0,\rho) | \widetilde{0,\text{Min},t_2} \rangle = \int_{\omega>0} \frac{d\omega}{(2\pi)^2} \frac{1}{\omega} N_\omega^2 K_{i\omega}(m\rho) K_{-i\omega}(m\rho) 2\Re \left(\frac{e^{\pi\omega}(1-e^{2\pi\omega})}{(1-e^{-2\pi\omega - i\omega t_2})^2} \right) \tag{101}$$

Which again decreases with t_2. Now the field operator is time shifted with a dependence on the number of particles, and result is the same. Following appendix A.3 we can generalise this for higher powers of N_L. Moreover we can combine phase shifts of the form (94) with phase shifts of the form (98) and their higher power variants to obtain the general phases.
Like we stated in equation (77) the most general phases are given by:

$$|\widetilde{0,\text{Min},\delta(n,\omega)}\rangle = (1-e^{-2\pi\omega})^{\frac{1}{2}} \sum_{n=0}^{\infty} e^{-n\pi\omega} e^{-i\delta(n,\omega)} |n,L\rangle |n,R\rangle \tag{102}$$

This $\delta(n,\omega)$ needs to exist for all $\omega > 0$ and $n \in \mathbb{N}$. Therefore we require existence and non-singularity on the dependence of ω. For n we are only interested in the integer points therefore we can always draw a polynomial through these points. Thus we can rewrite the general phase $\delta(n,\omega)$ as:

$$\delta(n,\omega) = \theta_1(\omega)n + \theta_2(\omega)n^2 + \dots \tag{103}$$

We can reinterpret this phase as induced by an operator:

$$U = e^{-i\left(\theta_1(\omega)N_L + \theta_2(\omega)N_L^2 + \dots\right)} \tag{104}$$

Which, like as we did before, is used to change the operators instead of the state. This will smear the operator in the time direction, furthermore the two point function will decrease. This, however, is most easily seen from the work we did before.
Therefore every phase in equation (77) can be reinterpreted as some sort of time shift of the left wedge leaving the right wedge invariant, or vice versa. Barring special cases, the left and right wedge separate as both the geodesic distance increases and the two-point functions containing both left and right wedge terms decrease.

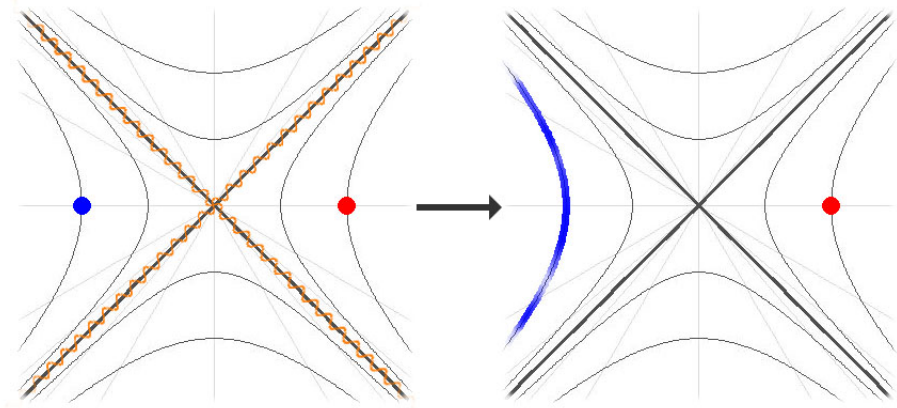

Figure 5: Phases in the Hartle-Hawking state can be removed by a non-trivial coordinate transformation on one wedge of Rindler space.

3.3 Local phase changes

If we are given a Hartle-Hawking state with phases, then we can remove the phases by coordinate transformations. These phases, and therefore the geometry of the space, are given from the start. A localized scientist or observer may interact with the state at some finite time. A localized observer does not have knowledge of the entire space. Therefore his operators will be incomplete, or flawed. We model his operators with a window function.

$$\tilde{O}(t) = e^{-t^2/T^2} O(t) \tag{105}$$

Where $\tilde{O}$ and $O(t)$ are the flawed operator and the normal operator respectively. We have used as window function e^{-t^2/T^2} because it is simple. However, we can construct more general window functions from this one. Moreover for convenience we will leave out normalization factors. We are more interested what happens to the Fourier space operators.

$$O(\omega) = \frac{1}{2\pi}\int_{-\infty}^{\infty} e^{-i\omega t} O(t) dt \tag{106}$$

$$\tilde{O}(\omega) = \frac{1}{2\pi}\int_{-\infty}^{\infty} e^{-i\omega t} \tilde{O}(t) dt \tag{107}$$

as an ansatz how the flawed Fourier operators are related to the normal Fourier we will use:

$$\tilde{O}(\omega) = \int_{-\infty}^{\infty} f(\omega, \omega') O(\omega') d\omega' \tag{108}$$

we plug this and (105) in (107) and obtain:

$$\tilde{O}(\omega) = \frac{1}{2\pi}\int_{-\infty}^{\infty} e^{-i\omega t} \tilde{O}(t) dt \tag{109}$$

$$\int_{-\infty}^{\infty} f(\omega, \omega') O(\omega') d\omega' = \frac{1}{2\pi}\int_{-\infty}^{\infty} e^{-i\omega t} e^{-t^2/T^2} O(t) dt \tag{110}$$

$$\frac{1}{2\pi}\int_{-\infty}^{\infty}\int_{-\infty}^{\infty} f(\omega, \omega') e^{-i(\omega'-\omega)t} d\omega' e^{-i\omega t} O(t) dt = \frac{1}{2\pi}\int_{-\infty}^{\infty} e^{-t^2/T^2} e^{-i\omega t} O(t) dt \tag{111}$$

Therefore we find that:

$$\int_{-\infty}^{\infty} f(\omega, \omega') e^{-i(\omega'-\omega)t} d\omega' = e^{-t^2/T^2} \tag{112}$$

Thus the inverse Fourier transform of $f(\omega, \omega')$ is of Gaussian shape. Therefore $f(\omega, \omega')$ is of Gaussian shape. So we obtain:

$$\tilde{O}(\omega) = T\int_{0}^{\infty} e^{-T^2(\omega'-\omega)^2/4} O(\omega') d\omega' \tag{113}$$

adding in the normalization may scale future results, however, their behaviour does not change. Moreover the operators we are interested in only exists for $\omega > 0$ thus the lower bound of the integral is zero. The creation and annihilation operators are Fourier operators and their flawed variants behaves as stated above. A localized observed can most easily study physics with two-point functions.

$$\langle 0, \text{Min}| \tilde{a}^\dagger(\omega_1)\tilde{a}(\omega_2) |0, \text{Min}\rangle = T^2 \iint_0^\infty e^{-T^2(\omega_1'-\omega_1)^2/4} e^{-T^2(\omega_2'-\omega_2)^2/4} \langle 0, \text{Min}| a^\dagger(\omega_1')a(\omega_2') |0, \text{Min}\rangle \, d\omega_1' d\omega_2' \tag{114}$$

$$= T^2 \iint_0^\infty e^{-T^2(\omega_1'-\omega_1)^2/4} e^{-T^2(\omega_2'-\omega_2)^2/4} \frac{1}{e^{2\pi\omega_1'} - 1} \delta(\omega_1' - \omega_2') d\omega_1' d\omega_2' \tag{115}$$

Which is non-zero for $\omega_1 \neq \omega_2$. We are interested whether a local scientist can change the phases of the Hartle-Hawking state using these flawed operators.

$$|\widetilde{0, \text{Min}}\rangle = U(t) |0, \text{Min}\rangle \tag{116}$$

Where $U(t) = e^{i\omega N_\omega t}$. We need the commutation relations of the flawed operators to study this state.

$$[\tilde{a}(\omega_1), \tilde{a}(\omega_2)] = 0 \tag{117}$$

However, the other one is more difficult.

$$[\tilde{a}^\dagger(\omega_1), \tilde{a}(\omega_2)] = T^2 \iint_0^\infty e^{-T^2(\omega_1'-\omega_1)^2/4} e^{-T^2(\omega_2'-\omega_2)^2/4} [a^\dagger(\omega_1'), a(\omega_2')] d\omega_1' d\omega_2' \tag{118}$$

$$= T^2 \iint_0^\infty e^{-T^2(\omega_1'-\omega_1)^2/4} e^{-T^2(\omega_2'-\omega_2)^2/4} \delta(\omega_1' - \omega_2') d\omega_1' d\omega_2' \tag{119}$$

$$\sim T e^{-T^2(\omega_1-\omega_2)^2/8} \left(1 - \text{erf}\left(-\frac{T(\omega_1+\omega_2)}{2\sqrt{2}}\right)\right) \tag{120}$$

$$\sim T e^{-T^2(\omega_1-\omega_2)^2/8} \tag{121}$$

We are only interested in the behaviour of this commutator, exact normalization and small factors like the error function do not affect the behaviour for large T. This commutator behaves as a delta function when send $T \to \infty$. We can calculate the commutator of the flawed number operator with one (or more) of the Fourier operators:

$$[\tilde{N}(\omega_1), \tilde{a}(\omega_2)] \sim T e^{-T^2(\omega_1-\omega_2)^2/8} \tilde{a}(\omega_2) \tag{122}$$

$$[\tilde{N}(\omega_1), \tilde{a}^\dagger(\omega_2)] \sim -T e^{-T^2(\omega_1-\omega_2)^2/8} \tilde{a}^\dagger(\omega_2) \tag{123}$$

Using this together the following combinatorial trick [7].

$$Be^{-A} = e^{-A}\left(B + [A,B] + \frac{1}{2!}[A,[A,B]] + \frac{1}{3!}[A,[A,[A,B]]] + ...\right) \tag{124}$$

We pass the creation and annihilation operators through the time evolution operator,

$$\tilde{a}(\omega_1)e^{-i\omega_2 N_{\omega_2} t} \sim e^{-i\omega_2 N_{\omega_2} t} \tilde{a}(\omega_1) \exp\left(i\omega_2 t T e^{-T^2(\omega_1-\omega_2)^2/8}\right) \tag{125}$$

$$\tilde{a}^\dagger(\omega_1)e^{-i\omega_2 N_{\omega_2} t} \sim e^{-i\omega_2 N_{\omega_2} t} \tilde{a}^\dagger(\omega_1) \exp\left(-i\omega_2 t T e^{-T^2(\omega_1-\omega_2)^2/8}\right) \tag{126}$$

and calculate the two-point function for the flawed operators for an one-sided time evolved state:

$$\langle\widetilde{0, \text{Min}}|\tilde{a}^\dagger(\omega_1)\tilde{a}(\omega_2)|\widetilde{0, \text{Min}}\rangle = \langle 0, \text{Min}| e^{i\omega_3 N_{\omega_3} t} \tilde{a}^\dagger(\omega_1)\tilde{a}(\omega_2) e^{-i\omega_3 N_{\omega_3} t} |0, \text{Min}\rangle \tag{127}$$

$$= \exp\left(i\omega_3 t T e^{-T^2(\omega_1-\omega_3)^2/8}\right) \exp\left(-i\omega_3 t T e^{-T^2(\omega_2-\omega_3)^2/8}\right) \tag{128}$$

$$\times \langle 0, \mathrm{Min}| \tilde{a}^{\dagger}(\omega_1)\tilde{a}(\omega_2) |0, \mathrm{Min}\rangle$$

A phase is detectable by the local scientist and the reduced density matrix is therefore changed after the time evolution. This state, after the time-evolution, cannot be represented by a Hartle-Hawking state with changed phases as that would leave the reduced density matrix unchanged. If we allow the local scientist greater and greater knowledge (sending $T \to \infty$) the reduced density matrix is not restored. On first sight sending $T \to \infty$ would restore equation (114) to its normal form. The two exponentials in the integral become delta functions and off-diagonal elements become zero. Furthermore the phases in equation (128) become zero. However at the same that we let $T \to \infty$ we should let in the Fourier space $\omega \to 0$ such that $T\omega =$ constant because longer time scales correspond to smaller frequency scales. Using this in equations (114),(128) restores the off-diagonal elements and the phase, showing that the reduced density matrix is still changed by this time evolution and can ,therefore, not affect the phases like the operations discussed in the previous sections.
Once we remove the phases as we did in section 3.2, they are removed for all time and a local scientist cannot change the phases again without changing the reduced density matrix on his side.

4 An explicit example: The BTZ black hole

The idea that a black hole can be described by an entangled state can be made more precise in the framework of AdS/CFT. With AdS/CFT we can relate fields inside AdS space to a CFT living on the boundary. Maldacena proposed that a black hole could be dual to two CFTs [4], each describing one wedge outside the black hole and together describing the inside of a black hole. As a specific example of this double duality we will study the BTZ black hole.

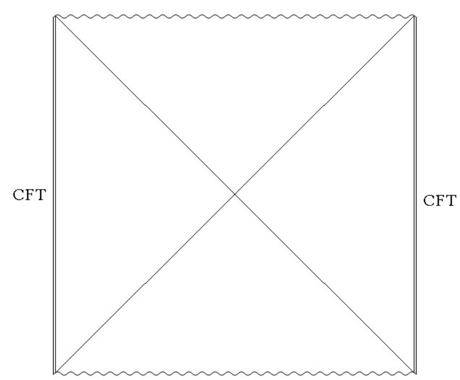

Figure 6: Penrose diagram of the BTZ black hole. Maldacena's proposal places a CFT on either side of the black hole [4].

4.1 BTZ black hole metric

The BTZ black hole metric is given by.

$$ds^2 = -(r^2 - r_0^2)dt^2 + (r^2 - r_0^2)^{-1}dr^2 + r^2dx^2 \tag{129}$$

This metric is a solution of the Einstein equations in 2+1 dimensions. Moreover we clearly see the behaviour of a black hole metric. For $r < r_0$ the time coordinated becomes space like and the space coordinate becomes time like. And at $r = r_0$ we encounter a coordinate singularity, just like we are used to for a Schwarzschild black hole. Furthermore if we make the following coordinates transformation: $\epsilon = r - r_0$ and look close to the horizon $\epsilon << r_0$ we obtain:

$$ds^2 = -2r_0\epsilon dt^2 + (2r_0\epsilon)^{-1}d\epsilon^2 + r_0^2d\phi^2 \tag{130}$$

Now we set $\rho = 2\sqrt{2r_0\epsilon}$ and $t = r_0\tau$. Moreover we ignore the dx^2 term, which is merely extra dimension. We get:

$$ds^2 = -\rho^2 d\tau^2 + d\rho^2 \tag{131}$$

the Rindler metric. Although we do not want to work in the approximation to the near horizon region which is Rindler space, we can use this result to obtain a the temperature of the black hole:

$$\beta = \frac{2\pi}{r_0} \tag{132}$$

The BTZ black hole we study is also a little different from the well known Schwarzschild black hole. The BTZ black hole is planar and not spherical. Moreover at $r = 0$ there is no singularity like in the case of the Schwarzschild black hole.
We want to study the BTZ black hole without making the approximation to Rindler space. The most useful method to study the BTZ space-time is the AdS/CFT correspondence. Letting $r \to \infty$ we obtain the following.

$$ds^2 = -r^2 dt^2 + r^{-2} dr^2 + r^2 dx^2 \tag{133}$$

now setting $r = \frac{1}{z}$ we get:

$$ds^2 = \frac{-dt^2 + dz^2 + dx^2}{z^2} \tag{134}$$

Which is the metric of AdS_3, thus the BTZ space is asymptotically AdS. Therefore we can use our tools of AdS/CFT. A difference to the normal treatment of AdS/CFT is that there are two CFTs, another is that these CFTs reflect the thermal state of a black hole and are at a finite temperature.

4.2 Two-point function of a CFT on $\mathbb{R}^2$

As before we want to work with a free scalar field of mass m, this corresponds with a CFT with a conformal dimension of:

$$\Delta = \frac{d}{2} + \sqrt{\frac{d^2}{4} + m^2} \tag{135}$$

The most useful tool for CFTs are two-point functions. To obtain the two-point function we make use of the many symmetries of a CFT.

$$\langle O(x, y) O(x', y') \rangle = g(x, x', y, y') \tag{136}$$

Using translational and rotational invariance we see that:

$$g(x, x', y, y') = g\left(\sqrt{(x - x')^2 + (y - y')^2}\right) = g(s) \tag{137}$$

Where $s^2 = (x - x')^2 + (y - y')^2$. Furthermore we have the scaling $O(\lambda x, \lambda y) = \lambda^\Delta O(x, y)$. Which leads to:

$$g(\lambda s) = \langle O(\lambda x, \lambda y) O(\lambda x', \lambda y') \rangle \tag{138}$$
$$= \lambda^{2\Delta} g(s) \tag{139}$$

There is an unique function that solves this scaling law.

$$g(s) = \frac{c}{s^{2\Delta}} = \frac{c}{((x - x')^2 + (y - y')^2)^\Delta} \tag{140}$$

Where c is some arbitrary constant. Although we set $c = 1$ for our calculations at this point, we should remember that we have the freedom to choose c however we want. This could be useful for normalization further on. For now we we will use:

$$\langle O(x, y) O(x', y') \rangle = \frac{1}{((x - x')^2 + (y - y')^2)^\Delta} \tag{141}$$

In a similar manner three point function can be obtained.

4.3 Two-point function of a CFT on $\mathbb{R} \times \mathbb{S}$

For the study of a CFT with at a non zero temperature, it is necessary to obtain the two-point function on a cylinder. Therefore we need

$$\langle O(x,y)O(x',y')\rangle_{2\pi} \tag{142}$$

Where the 2π is the circumference of the circle. We start with the unit circle and can scale when we need another circumference. We need to map $\mathbb{R}^2 \to \mathbb{R} \times \mathbb{S}$, for which we will use:

$$z \ = x + iy \tag{143}$$

$$z' = \ln(z) \tag{144}$$

$$z' = u + iv \tag{145}$$

It is easy to show that this maps the plane to a cylinder by writing $z = re^{i\theta} \Rightarrow z' = \ln(z) = \ln(r) + i\theta$, where $\ln(r)$ is now the longitudinal coordinate and θ is the angular coordinate. This mapping is analytic everywhere except for the branch at $z = 0$, furthermore it has branch cut which can be chosen along the positive real axis such that θ runs from zero to 2π (which leads to the circumference of 2π).We can avoid the branch point using the translational invariance such that our coordinates in the two-point function are non-zero. Furthermore we will shift our coordinates such that $x, x' > 0$, this will simplify our calculations. The mapping $z' = \ln(z)$ leads to the coordinate mapping:

$$u = \frac{1}{2}\ln(x^2 + y^2) \tag{146}$$

$$v = \arctan(y/x) \tag{147}$$

$$x = e^u(1 + \tan^2(v))^{-\frac{1}{2}} = e^u \sin(v) \tag{148}$$

$$y = e^u(1 + \cot^2(v))^{-\frac{1}{2}} = e^u \cos(v) \tag{149}$$

Therefore we can rewrite the two-point function on the cylinder in terms of the two-point function on the plane.

$$\langle O(u,v)O(u',v')\rangle_{2\pi} = \frac{\partial(x,y)}{\partial(u,v)}^{\Delta/2} \frac{\partial(x',y')}{\partial(u',v')}^{\Delta/2} \langle O(x,y)O(x',y')\rangle \tag{150}$$

$$= (e^u e^{u'})^{\Delta} \frac{1}{((x-x')^2 + (y-y')^2)^{\Delta}} \tag{151}$$

$$= \frac{1}{(e^{u-u'} + e^{u'-u} - 2\cos(v - v'))^{\Delta}} \tag{152}$$

We simplify this using translational invariance.

$$\langle O(u,v)O(0,0)\rangle_{2\pi} = \frac{1}{(2\cosh(u) - 2\cos(v))^{\Delta}} \tag{153}$$

$$\langle O(x,\tau)O(0,0)\rangle_{2\pi} = \frac{1}{(2\cosh(x) - 2\cos(\tau))^{\Delta}} \tag{154}$$

Where $x = u$ the longitudinal coordinate on the cylinder and $\tau = v$ the angular coordinate. Therefore we have obtained the two-point function on the cylinder.

4.4 Two-point function of a CFT at finite temperature on $\mathbb{R}^{1+1}$

When we interpret the angular coordinate as (periodic and euclidean) time, we can wick rotate to real time using $\tau = i(1 - i\epsilon)t$. After this rotation we obtain the in real time with an inverse temperature equal to the circumference of the circle, as explained in appendix A.1.

$$\langle O(x,t)O(0,0)\rangle_{2\pi} = \frac{1}{(2\cosh(x) - 2\cos(i(1 - i\epsilon)t))^{\Delta}} \tag{155}$$

$$= \frac{1}{(2\cosh(x) - 2\cosh((1-i\epsilon)t))^{\Delta}} \tag{156}$$

To put the system at inverse temperature $\beta = 1/T$ we scale the system with $\beta/2\pi$. Using the symmetries we obtain (setting ϵ to zero for simplicity):

$$\langle O(x,t)O(0,0)\rangle_{\beta} = \left(\frac{2\pi}{\beta}\right)^{2\Delta} \frac{1}{\left(2\cosh(\frac{2\pi}{\beta}x) - 2\cosh(\frac{2\pi}{\beta}t)\right)^{\Delta}} \tag{157}$$

In the case of the BTZ black hole Maldacena proposed that it is dual to two CFTs. Therefore we need to specify on which CFT these operators work. We will label the operators as either O_R or O_L. For the two-point function with both operators one side the result is the same as above. If one of the operators is on one side and one on the other we need to analytically continue $t \to t + i\beta/2$ to obtain the mixed two-point function.

$$\langle O_L(x,t)O_R(0,0)\rangle_{\beta} = \left(\frac{2\pi}{\beta}\right)^{2\Delta} \frac{1}{\left(2\cosh(\frac{2\pi}{\beta}x) + 2\cosh(\frac{2\pi}{\beta}t)\right)^{\Delta}} \tag{158}$$

We need to be careful with coordinate shifts. as the two operators work on different systems their coordinates are different sets. For the space coordinates there is little trouble, translation work as expected from the notation above. We can do the same for the time coordinate, the time is a Killing vector in this case. This leads to time flowing 'backward' in the Penrose diagram. In this convention all patches in the Penrose diagram are continuously connected by the time, so it is a 'natural' choice. It is a choice and one can study the effect of letting the time run the other way, like we did for Rindler space in section 3.1. For our notation we assume that we follow the Killing vector, thus time flowing against the killing vector on one side would be denoted by, for example $O_L(x,-t)$. When we exchange left with right nothing changes, so we only need to consider one two-point function with both operators on one side and one mixed two-point function.

4.5 Two-point function of the Fourier operators

To solve most problems we need the Fourier transform of the two-point function. The Fourier operators are given by the Fourier transform:

$$\tilde{O}_R(k,\omega) = \frac{1}{2\pi}\int_{-\infty}^{\infty} e^{-i\omega t - ikx} O_R(x,t)dxdt \tag{159}$$

and $\tilde{O}_R^{\dagger}(k,\omega)$ is given by conjugation. Again our operators only exist for $\omega > 0$. Now we can construct the two-point functions in Fourier space.

$$\langle \tilde{O}_R(k,\omega)\tilde{O}_R(k',\omega')\rangle_{\beta} = \frac{1}{(2\pi)^2}\int_{-\infty}^{\infty} e^{-i\omega t - ikx - i\omega' t' - ik'x'} \langle O_R(x,t)O_R(x',t')\rangle_{\beta} dxdtdx'dt' \tag{160}$$

$$= \int_{-\infty}^{\infty} e^{-i\omega t - ikx}\langle O_R(x,t)O_R(0,0)\rangle_{\beta} dxdt\delta(\omega+\omega')\delta(k+k') \tag{161}$$

As $\omega, \omega' > 0$ the delta function will give zero, however, as the other two-point functions are very similar we continue with the calculation. It easier to work with light cone coordinates as this simplifies the two-point function.

$$u = x - t \tag{162}$$

$$v = x + t \tag{163}$$

$$k_u = \frac{1}{2}(k - \omega) \tag{164}$$

$$k_v = \frac{1}{2}(k + \omega) \tag{165}$$

We then obtain:

$$\langle O_R(u,v) O_R(0,0)\rangle_\beta = \left(\frac{2\pi}{\beta}\right)^{2\Delta} \frac{2^\Delta}{\left(2\cosh(\frac{2\pi}{\beta}\frac{1}{2}(u-v)) - 2\cosh(\frac{2\pi}{\beta}\frac{1}{2}(u+v))\right)^\Delta} \tag{166}$$

$$= \left(\frac{2\pi}{\beta}\right)^{2\Delta} \frac{2^\Delta}{\left(4\sinh(\frac{\pi}{\beta}u)\sinh(-\frac{\pi}{\beta}v)\right)^\Delta} \tag{167}$$

The same applies to the mixed two-point function.

$$\tag{168}$$

$$\langle O_L(u,v) O_R(0,0)\rangle_\beta = \left(\frac{2\pi}{\beta}\right)^{2\Delta} \frac{2^\Delta}{\left(4\cosh(\frac{\pi}{\beta}u)\cosh(\frac{\pi}{\beta}v)\right)^\Delta} \tag{169}$$

Applying this to our integral:

$$\int_{-\infty}^{\infty} e^{-i\omega t - ikx} \langle O_R(x,t) O_R(0,0)\rangle_\beta dx dt = -2^{\Delta+1} \int_{-\infty}^{\infty} e^{-ik_u u - ik_v v} \langle O_R(u,v) O_R(0,0)\rangle_\beta du dv \tag{170}$$

$$= -2^{\Delta+1}\left(\frac{\pi}{\beta}\right)^{2\Delta} \int_{-\infty}^{\infty} \frac{e^{-ik_u u}}{\left(\sinh(\frac{\pi}{\beta}u)\right)^\Delta} du \int_{-\infty}^{\infty} \frac{e^{-ik_v v}}{\left(\sinh(-\frac{\pi}{\beta}v)\right)^\Delta} dv \tag{171}$$

And obtain (through similar steps) the following two-point function for the Fourier operators.

$$\langle \tilde{O}_R^\dagger(k,\omega)\tilde{O}_R(k',\omega')\rangle_\beta = \left(\frac{\pi}{\beta}\right)^{2\Delta} \frac{2^{2\Delta-1}\beta^2 e^{-\omega\beta/2}}{(2\pi i(\omega+k)\beta - \pi\Delta)(2\pi i(k-\omega)\beta - \pi\Delta)}$$
$$\times \frac{\Gamma(1 - \frac{i(\omega+k)\beta}{4\pi} + \Delta/2)\Gamma(\frac{i(\omega+k)\beta}{4\pi} + \Delta/2)}{\Gamma(\Delta)}$$
$$\times \frac{\Gamma(1 - \frac{i(k-\omega)\beta}{4\pi} + \Delta/2)\Gamma(\frac{i(k-\omega)\beta}{4\pi} + \Delta/2)}{\Gamma(\Delta)} \delta(\omega-\omega')\delta(k-k') \tag{172}$$

This is not a very useful form. Setting $a = \frac{ik}{4\pi}\beta$ and $b = \frac{i\omega}{4\pi}\beta$ and using some Gamma function identities we obtain:

$$\langle \tilde{O}_R^\dagger(k,\omega)\tilde{O}_R(k',\omega')\rangle_\beta = \left(\frac{\pi}{\beta}\right)^{2\Delta} \frac{2^{2\Delta}\beta}{2\pi}\frac{1}{\omega}\frac{1}{e^{\omega\beta}-1}$$
$$\times \frac{\Gamma(-a-b+\Delta/2)\Gamma(a+b+\Delta/2)}{\Gamma(2b)\Gamma(\Delta)}$$
$$\times \frac{\Gamma(-a+b+\Delta/2)\Gamma(a-b+\Delta/2)}{\Gamma(-2b)\Gamma(\Delta)} \delta(\omega-\omega')\delta(k-k') \tag{173}$$

This is still not a very useful form. However, we can now recognise the part $\frac{1}{e^{\omega\beta}-1}$. Which is the occupation density of a temperature $T = 1/\beta$. The first part are merely constants, and as said in section 4.2 we still have the freedom multiply our operators with any constant. Therefore we redefine our operators as follows, forgetting about the constants:

$$\tilde{O}_R(k,\omega) = \frac{1}{\sqrt{\omega}}\frac{1}{\Gamma(\Delta)}\sqrt{\frac{\Gamma(a+b+\Delta/2)\Gamma(a-b+\Delta/2)\Gamma(-a+b+\Delta/2)\Gamma(-a-b+\Delta/2)}{\Gamma(2b)\Gamma(-2b)}} a_R(k,\omega) \tag{174}$$

The other operators are redefined in similar manner. These new operators have relatively simple two-point functions:

$$\langle a_R^\dagger(k,\omega)a_R(k',\omega')\rangle_\beta = \frac{1}{e^{\omega\beta}-1}\delta(\omega-\omega')\delta(k-k') \tag{175}$$

$$\langle a_R(k,\omega)a_R^\dagger(k',\omega')\rangle_\beta = \frac{e^{\omega\beta}}{e^{\omega\beta}-1}\delta(\omega-\omega')\delta(k-k') \tag{176}$$

$$\langle a_L(k,\omega)a_R(k',\omega')\rangle_\beta = \frac{1}{e^{\omega\beta/2}-e^{-\omega\beta/2}}\delta(\omega-\omega')\delta(k-k') \tag{177}$$

$$\langle a_L^\dagger(k,\omega)a_R^\dagger(k',\omega')\rangle_\beta = \frac{1}{e^{\omega\beta/2}-e^{-\omega\beta/2}}\delta(\omega-\omega')\delta(k-k') \tag{178}$$

The other two point functions are zero or equivalent to one of these. From these two-point functions we can also obtain the commutation relations.

$$[a_R(k,\omega), a_R^\dagger(k',\omega')] = \delta(\omega-\omega')\delta(k-k') \tag{179}$$

The other commutation relations are equivalent to this one or they are zero. For the bulk field operator within the BTZ space we need to connect at the boundary with the true CFT operators (the O's). For calculations these $a(k,\omega), a^\dagger(k,\omega)$ are more useful. Therefore we include $\frac{1}{\sqrt{\omega}}$ in the construction of the bl field operator, while we include rest of equation (174) in the interior wave mode.

4.6 BTZ interior modes

To obtain the interior wave mode we place a scalar field with mass m on the background of the BTZ metric. This field obeys the Klein-Gordon equation (25).

$$\Box\psi = m^2\psi \tag{180}$$

Similar as in the Rindler case this becomes in a curved background:

$$\frac{1}{\sqrt{-g}}\partial_\mu\sqrt{-g}g^{\mu\nu}\partial_\nu\psi = m^2\psi \tag{181}$$

Where $g_{\mu\nu}$ is the metric and g is the determinant of the metric. With the metric given by (129), equation (181) becomes:

$$\left(\frac{-1}{r^2-r_0^2}\frac{\partial^2}{\partial t^2} + \frac{1}{r^2}\frac{\partial^2}{\partial\phi^2} + \frac{1}{r}\frac{\partial}{\partial r}r(r^2-r_0^2)\frac{\partial}{\partial r}\right)\psi = m^2\psi \tag{182}$$

Using the translational freedom of t and rotational freedom of ϕ, we can make the following substitution:

$$\psi = e^{-i\omega t}e^{ikx}f_{\omega,k}(r) \tag{183}$$

where $\omega > 0$ and $k \in \mathbb{Z}$. And obtain the equation for $f_{\omega,k}(r)$.

$$\left(\frac{\omega^2}{r^2-r_0^2} - \frac{k^2}{r^2} - m^2\right)f_{\omega,k}(r) + \left(3r - \frac{r_0^2}{r}\right)f'_{\omega,k}(r) + \left(r^2-r_0^2\right)f''_{\omega,k}(r) = 0 \tag{184}$$

this has the following solutions:

$$f_{1\,k,\omega}(r) = \left(\frac{r^2}{r_0^2}\right)^a\left(\frac{r^2}{r_0^2}-1\right)^{+b}{}_2F_1\left(1+a+b-\Delta/2, a+b+\Delta/2, 1+2b, 1-\frac{r^2}{r_0^2}\right) \tag{185}$$

$$f_{2\,k,\omega}(r) = \left(\frac{r^2}{r_0^2}\right)^a\left(\frac{r^2}{r_0^2}-1\right)^{-b}{}_2F_1\left(1+a-b-\Delta/2, a-b+\Delta/2, 1-2b, 1-\frac{r^2}{r_0^2}\right) \tag{186}$$

where $a = \frac{ik}{2r_0}$ and $b = \frac{i\omega}{2r_0}$. There is a freedom in choosing the sign of a and b, this used to obtain the second independent solution. The other possibilities are obtained as the hermitian conjugate of these solution. Both these solutions are non-normalizable, therefore we must find the linear combination that is normalizable. We obtain:

$$f_{R\,k,\omega}(r) = N_R \left(\frac{r^2}{r_0^2}\right)^a \left(\frac{r^2}{r_0^2} - 1\right)^{-a-\Delta/2} {}_2F_1\left(a - b + \Delta/2, a + b + \Delta/2, \Delta, \frac{r_0^2}{r_0^2 - r^2}\right) \tag{187}$$

We have denoted this mode with subscript R as this will be the mode in the right universe. The hypergeometric function has the argument $\frac{r_0^2}{r_0^2-r^2}$ which is < 0 for $r > r_0$ therefore we cannot use the standard definition of the hypergeometric function. Although the hypergeometric function has a analytic continuation outside the argument $[0, 1]$, we transform the mode such that we can use it with the more basic definition.

$$f_{R\,k,\omega}(r) = N_R \left(\frac{r^2}{r_0^2}\right)^{b-\Delta/2} \left(\frac{r^2}{r_0^2} - 1\right)^{-b} {}_2F_1\left(a - b + \Delta/2, -a - b + \Delta/2, \Delta, \frac{r_0^2}{r^2}\right) \tag{188}$$

We have used in these last to equation N_R as the normalization factor. The bulk field operator has the following form:

$$\Psi_R(t, x, r) = \int_{\omega>0} \frac{d\omega dk}{(2\pi)^2} \Big(a_R(k, \omega)\psi_{R\,k,\omega}(t, x, r) + \text{h.c.}\Big) \tag{189}$$

Furthermore we need to connect to the CFT on the boundary:

$$\lim_{r\to\infty} \Psi(t, x, r) \sim r^{-\Delta} O(t, x) \tag{190}$$

Where $O(t, x)$ is the operator discussed in sections 4.2-4.4. Calculations are simpler using the operators defined in the last section. Therefore we take into account equation (174), thus our normalizable mode is

$$\begin{aligned} f_{R\,k,\omega}(r) =& \frac{1}{\sqrt{r_0}} \frac{1}{\Gamma(\Delta)} \sqrt{\frac{\Gamma(a + b + \Delta/2)\Gamma(a - b + \Delta/2)\Gamma(-a + b + \Delta/2)\Gamma(-a - b + \Delta/2)}{\Gamma(2b)\Gamma(-2b)}} \\ &\times \left(\frac{r^2}{r_0^2}\right)^{b-\Delta/2} \left(\frac{r^2}{r_0^2} - 1\right)^{-b} {}_2F_1\left(a - b + \Delta/2, -a - b + \Delta/2, \Delta, \frac{r_0^2}{r^2}\right) \end{aligned} \tag{191}$$

For the left universe we have a similar expression, we should take not note that the coordinates t and r are different from the coordinates used in the right universe. Furthermore as the time runs backward relative to the right universe the ansatz is $\psi = e^{i\omega t} e^{ikx} f_{\omega,k}(r)$. For the modes within the black hole, we cannot talk about normalizable or non-normalizable modes as we can not look at there behaviour when $r \to \infty$ as they are confined to be within the black hole. Therefore we use the modes (185) and (186) to construct the bulk field operator within the black hole.

$$\Psi_{BH}(t, x, r) = \int_{\omega>0} \frac{d\omega dk}{(2\pi)^2} \Big(b_1(k, \omega)\psi_{1\,k,\omega}(t, x, r) + b_2(k, \omega)\psi_{2\,k,\omega}(t, x, r) + \text{h.c.}\Big) \tag{192}$$

Where

$$\psi_{1\,k,\omega}(t, x, r) = e^{-i\omega t} e^{ikx} N_1 \left(\frac{r^2}{r_0^2}\right)^a \left(\frac{r^2}{r_0^2} - 1\right)^{+b} {}_2F_1\left(1 + a + b - \Delta/2, a + b + \Delta/2, 1 + 2b, 1 - \frac{r^2}{r_0^2}\right) \tag{193}$$

$$\psi_{2\,k,\omega}(t, x, r) = e^{-i\omega t} e^{ikx} N_2 \left(\frac{r^2}{r_0^2}\right)^a \left(\frac{r^2}{r_0^2} - 1\right)^{-b} {}_2F_1\left(1 + a - b - \Delta/2, a - b + \Delta/2, 1 - 2b, 1 - \frac{r^2}{r_0^2}\right) \tag{194}$$

Now we have constructed the bulk field operators in the all regions. We have two sets of operators a_R, a_L and b_1, b_2, where we only need one set to describe the field.

4.7 Behind the horizon

To link one set of operators to the other, we look at heir behaviour near the horizon. For the near horizon expansion we introduce the tortoise coordinate:

$$r_* = \frac{1}{2r_0}\log\left(\frac{r-r_0}{r+r_0}\right) \tag{195}$$

Using the $z \to 1$ expansion for the hypergeometric function, we obtain the following expansion near the horizon.

$$f_{R\,k,\omega}(r) = r_0^{-1/2}\left(e^{i\delta}e^{i\omega r_*} + e^{-i\delta}e^{-i\omega r_*}\right) \tag{196}$$

Where

$$e^{i\delta} = 4^b\sqrt{\frac{\Gamma(-2b)\Gamma(a+b+\Delta/2)\Gamma(-a+b+\Delta/2)}{\Gamma(2b)\Gamma(-a-b+\Delta/2)\Gamma(a-b+\Delta/2)}} \tag{197}$$

Again using light-cone coordinates simplify our calculations.

$$v = r_* + t \tag{198}$$

$$u = -r_* + t \tag{199}$$

For the right universe, Setting $x = 0$ our bulk field operators are;

$$\Psi_{BH}(t,x,r) = \int_{\omega>0}\frac{d\omega dk}{(2\pi)^2}\left(b_1(k,\omega)N_1e^{i\omega u} + b_2(k,\omega)N_2e^{-i\omega v} + \text{h.c.}\right) \tag{200}$$

$$\Psi_R(t,x,r) = \int_{\omega>0}\frac{d\omega dk}{(2\pi)^2}\left(a_R(k,\omega)\frac{1}{\sqrt{r_0}}(e^{i\delta}e^{-i\omega u} + e^{-i\delta}e^{-i\omega v}) + \text{h.c.}\right) \tag{201}$$

$$\Psi_L(t,x,r) = \int_{\omega>0}\frac{d\omega dk}{(2\pi)^2}\left(a_R(k,\omega)\frac{1}{\sqrt{r_0}}(e^{i\delta}e^{-i\omega v} + e^{-i\delta}e^{-i\omega u}) + \text{h.c.}\right) \tag{202}$$

When we approach the horizon in the right universe we see that $t \to \infty$ and $r_* \to -\infty$. We can choose to take the path that leaves $r_* + t = v$ constant. The terms with u start to rotate very rapidly and by virtue of the Riemann-Lebesgue lemma do not contribute to the integral. Therefore we remain with:

$$\Psi_{BH}(t,x,r) = \int_{\omega>0}\frac{d\omega dk}{(2\pi)^2}\left(b_2(k,\omega)N_2e^{-i\omega v} + \text{h.c.}\right) \tag{203}$$

$$\Psi_R(t,x,r) = \int_{\omega>0}\frac{d\omega dk}{(2\pi)^2}\left(a_R(k,\omega)\frac{1}{\sqrt{r_0}}e^{-i\delta}e^{-i\omega v} + \text{h.c.}\right) \tag{204}$$

And we conclude that, by analytic continuation that:

$$a_R = b_2 \tag{205}$$

$$N_2 = \frac{1}{\sqrt{r_0}}e^{-i\delta} \tag{206}$$

Similarly for the left universe we approach the black hole with u constant and obtain:

$$a_L = b_1^\dagger \tag{207}$$

$$N_1 = \frac{1}{\sqrt{r_0}}e^{i\delta} \tag{208}$$

Therefore we are in the same situation as in the Rindler case. The inside of the black hole (future wedge) is described by analytic continuation of the left and right universes.

4.8 Hartle-Hawking state

We can talk about the state of a black hole because both the inside and outside of the black hole are described by the same set of operators. Otherwise we would have two states, one for the inside of the black hole and one for the outside. Therefore the black hole state can be written as a state of the left and right systems. In the basis of the number of particles:

$$|\text{BH}\rangle = \sum_{m,n} c_{m,n} |m, L\rangle |n, R\rangle \tag{209}$$

Instead of not allowing states with a negative number of particles we will set the constant in front of them zero. Furthermore we already know the two-point functions of the annihilation and creation operators, see section 4.5. Working out how the creation and annihilation operators interact with this state and comparing with (175)-(178), we get:

$$|\text{BH}\rangle = (1 - e^{-\beta\omega})^{\frac{1}{2}} \sum_{n=0}^{\infty} e^{-n\omega\beta/2} |n, L\rangle |n, R\rangle \tag{210}$$

The same as the Rindler state corresponding to the Minkowski vacuum, only the temperature is different. More precisely it is the Hartle-Hawking state.
As we did before we can compare the two-point function with the geodesic distance. The geodesic distance is given by[8]:

$$\cosh(d) = T_1 T_1' + T_2 T_2' - X_1 X_1' - X_2 X_2' \tag{211}$$

where

$$T_1 = \frac{1}{r_0}\sqrt{r^2 - r_0^2}\sinh(r_0 t) \tag{212}$$

$$X_1 = \frac{1}{r_0}\sqrt{r^2 - r_0^2}\cosh(r_0 t) \tag{213}$$

$$T_2 = \frac{r}{r_0}\cosh(r_0 x) \tag{214}$$

$$X_2 = \frac{r}{r_0}\sinh(r_0 x) \tag{215}$$

To go to from the right to the left region we use $t \to t + i\beta/2$. we can calculate the distance between the two CFTs by using $r, r' \to \infty$, thus $\cosh(d) \approx e^d/2$.

$$e^d \approx \frac{rr'}{r_0^2}\Big(2\cosh\big(r_0(x - x')\big) + 2\cosh\big(r_0(t - t')\big)\Big) \tag{216}$$

at the same time the two-point function behaves as (using both equations (190) and (158)):

$$\langle \Psi_R(t, x, r)\Psi_L(t', x', r')\rangle \sim \langle r^{-\Delta} O_R(t - t', x - x') r'^{-\Delta} O_L(0, 0)\rangle \tag{217}$$

$$\sim \frac{r^{-\Delta} r'^{-\Delta}}{\big(2\cosh\big(r_0(x - x')\big) + 2\cosh(r_0(t - t'))\big)^{\Delta}} \tag{218}$$

For large m we can use the connection between the geodesic distance and the two-point function explained in appendix A.2, moreover $\Delta \approx m$ in this case.

$$\langle \Psi_R(t, x, r)\Psi_L(t', x', r')\rangle \sim \left(\frac{rr'}{r_0^2}\big(2\cosh\big(r_0(x - x')\big) + 2\cosh(r_0(t - t'))\big)\right)^{-m} \approx e^{-md} \tag{219}$$

This connection to the geodesic distance makes two-point functions easier to compute. Therefore this tool is often used to compute two point functions.

4.9 Perturbed black hole: Phase changes

Although the two-point functions of heavy particles is easily calculated through the geometry of the space, we should be careful about what we know about the geometry of the black hole. The connection between geodesic distance and the two-point function holds also on small scales, only requiring large m. Therefore pertubations that affect the two-point function will also affect the geometry. Just like in the case of the Rindler space, we will perturb the system by adding phases to the Hartle-Hawking state:

$$|\text{BH}\rangle = (1-e^{-\beta\omega})^{\frac{1}{2}} \sum_{n=0}^{\infty} e^{-n\omega\beta/2} e^{i\delta(n,\omega)} |n,L\rangle |n,R\rangle \tag{220}$$

In the Rindler case it was clear why we first obtained the state without phases. In Minkowski space-time we know that the boundaries between the wedges are not special in any way, thus requiring smoothness across those boundaries provided a natural way to connect the left and right wedges. For the BTZ case we connected right to left by analytically continuing $t \to t + i\beta/2$. However, there no such thing requiring smoothness like the Minkowski space-time for the Rindler case. Moreover we secretly chose $t \to t + i\beta/2$ such that we would and up with the state without phases. However, looking at a state with changed phases, as a simple example:

$$\widetilde{|\text{BH}\rangle} = (1-e^{-\beta\omega})^{\frac{1}{2}} \sum_{n=0}^{\infty} e^{-n\omega\beta/2} e^{-i\omega n t_p} |n,L\rangle |n,R\rangle \tag{221}$$

Which corresponds to a time shift of only the left region with magnitude t_p. We are in the situation as we were in the Rindler case. We translate the phase change to a unitary operator and preform an action similar to time evolution with this operator. The see what happens to the operators we revisit the Fourier operators:

$$\tilde{O}_R(k,\omega) = \frac{1}{2\pi}\int_{-\infty}^{\infty} e^{-i\omega t - ikx} O_R(x,t) dx dt \tag{222}$$

$$\tilde{O}_L(k,\omega) = \frac{1}{2\pi}\int_{-\infty}^{\infty} e^{-i\omega t - ikx} O_L(x,t) dx dt \tag{223}$$

To obtain the left operator we analytically continued the right operator with $t \to t + i\beta/2$:

$$\tilde{O}_L(k,\omega) = \frac{1}{2\pi}\int_{-\infty}^{\infty} e^{-i\omega t - ikx} O_R(x,t+i\beta/2) dx dt \tag{224}$$

The time-shift in the bulk field operator is a multiplicative factor of $e^{-i\omega t_p}$, which we can absorb into the CFT operator:

$$e^{-i\omega t_p}\tilde{O}_L(k,\omega) = \frac{1}{2\pi}\int_{-\infty}^{\infty} e^{-i\omega (t+t_p - ikx} O_R(x,t+i\beta/2) dx dt \tag{225}$$

$$= \frac{1}{2\pi}\int_{-\infty}^{\infty} e^{-i\omega t - ikx} O_R(x,t+i\beta/2+t_p) dx dt \tag{226}$$

We can calculate the two-point function of the bulk field operators for this state (221) and see how it is affected by the phase change. For simplicity we will only calculate the two-point function for the case that $r', r \to \infty$:

$$\widetilde{\langle\text{BH}|}\Psi_R(t,x,r)\Psi_L(t',x',r')\widetilde{|\text{BH}\rangle} \sim \left(\frac{rr'}{r_0^2}\big(2\cosh\big(r_0(x-x')\big) + 2\cosh(r_0(t-t'-t_p))\big)\right)^{-m} \tag{227}$$

This no longer connects to the geodesic distance we calculated. When we use the following analytic continuation $t \to t + i\beta/2 + t_p$ instead of $t \to t + i\beta/2$ to go to the left CFT from the right one we end up with the state with phases (221). This can easily be seen in equation (226). Using the same continuation in the geodesic distance gives again:

$$\langle\widetilde{\mathrm{BH}}|\Psi_R(t,x,r)\Psi_L(t',x',r')|\widetilde{\mathrm{BH}}\rangle \sim e^{-m\tilde{d}} \tag{228}$$

Just like as in the Rindler case can this be generalised to to the general phases. We analytically continue with $t \to t + i\beta/2 + \theta(\omega, N_L)$ and expand $\theta(\omega, N_L)$ in a similar manner as in section 3.2. Again we lose a clear geometric interpretation of the resulting operators. The geodesic distance becomes dependent of ω and the number of particles, becoming smeared by these quantities.
Inside the black hole something similar happens as in the future wedge of Rindler space. The bulk field operators splits into two parts.

$$\Psi_{BH} = \Psi_1 + \Psi_2 \tag{229}$$

One of the two follows the right universe and the other follows the left universe. And again only cross terms are affected by whatever continuation between left and right we do.
It is important that the smearing caused by these phases in only in the time direction, therefore the singularity causes no problems for this description.

4.10 Perturbed black hole: Shock wave

Shenker and Stanford [8] found another way to perturb the black hole. They added a few particles on one side of the black hole. Although this does not leave that side of the black hole invariant, the other side is unchanged. Moreover, the addition of a few particles should not have significant impact on the geometry of the black hole. However, if a particle is released early enough, at $t = t_w$, it will cross the $t = 0$ slice with large proper energy:

$$E_p \sim \frac{E_b}{r_0} e^{r_0 t_w} \tag{230}$$

Where E_b is the energy at the boundary. A back-reaction to the metric should be included when this is very large. We construct a shockwave of infalling null matter, with energy density E at the boundary. For simplicity we assume that the shock wave falls directly into the black hole, therefore we use that it is planar in the x direction. A light-cone coordinate variant of the metric is more useful as null matter travels with the speed of light.

$$ds^2 = \frac{-4dudv + r_0^2(1-uv)^2 dx^2}{(1+uv)^2} \tag{231}$$

is the Kruskal form of the BTZ metric. A shockwave released at $t = t_w$ in the left universe will travel at constant $u_w = e^{-r_0 t_w}$. The black hole will grow, $\tilde{r}_0 = \sqrt{\frac{M+E}{M}} r_0$ where M is the mass density of the black hole. Therefore we will have two sets of coordinates, u, v to the right of the shockwave and $\tilde{u}, \tilde{v}$ to the left of the shockwave. Time must flow continuously therefore the shockwave travels along $\tilde{u}_w = e^{-\tilde{r}_0 t_w}$ in these new coordinates. Furthermore, the energy density of the shockwave is the same in both systems. Therefore the the g_{xx} components of both metrics should be equal at the shockwave.

$$\tilde{r}_0 \frac{1-\tilde{u}_w\tilde{v}}{1+\tilde{u}_w\tilde{v}} = r_0 \frac{1-u_w v}{1+u_w v} \tag{232}$$

For $E \ll M$, the two coordinate systems are related by:

$$\tilde{u} = u \tag{233}$$

$$\tilde{v} = v + \alpha \qquad\qquad \alpha = \frac{E}{4M} e^{r_0 t_w} \tag{234}$$

In the case that $E/M \to 0$ while $t_w \to \infty$ such that α remains constant, we have that $\tilde{r}_0 = r_0$ and we can write the metric of the entire space as:

$$ds^2 = \frac{-4dudv + (1 - u(v + \alpha\theta(u)))^2 dx^2}{(1 + u(v + \alpha\theta(u)))^2} \tag{235}$$

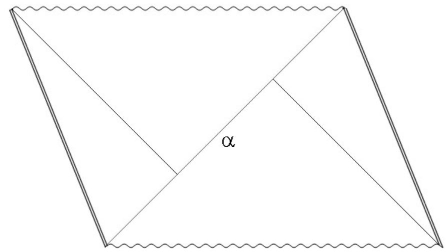

Figure 7: Penrose diagram of the BTZ black hole with a shock wave from the left [8]. The horizons miss by α

Where θ is the Heaviside step function.
The geometry of this metric is continues even though its derivatives are not. Therefore locally there are no large invariants. There are however large non-local invariants. The geodesic distance between two point, one on either side of the shockwave, is affected. To obtain the geometric distance, we calculate the distance from both points to a point on the shockwave and minimize the result. For large r, r'

$$e^d \approx \frac{rr'}{r_0^2}\left(2\cosh\left(r_0(x-x')\right) + 2\cosh\left(r_0(t-t')\right) + \alpha/2e^{-r_0(t+t')/2}\right) \tag{236}$$

This perturbed black hole cannot be represented by phase changes to the Hartle-Hawking state because it is not invariant under time-evolution following the Killing field.

5 Generalizations

We have seen that the Hartle-Hawking state can be perturbed by adding phases without affecting the outside of the black hole. We were able to remove the phases by a coordinate change in Rindler space and for the BTZ black hole. In this section we study whether it possible to do this for other cases as well.

5.1 Spherical BTZ black hole

Last section we treated the planar BTZ black hole. More relevant to the study of 'real' black holes would be the spherical BTZ black hole. The metric of the spherical BTZ black hole is almost the same as the planar BTZ black hole.

$$ds^2 = -(r^2 - r_0^2)dt^2 + (r^2 - r_0^2)^{-1}dr^2 + r^2 d\phi^2 \tag{237}$$

For the angular direction we identify $\phi = \phi + 2\pi$. Therefore the boundary CFT's life on $\mathbb{R} \times \mathbb{S}$, a cylinder. For the construction of real thermal two-point function we would need to construct Euclidean two-point functions on $\mathbb{S} \times \mathbb{S}$, the torus. However, so far this has not been done. A lot of symmetry is lost on that geometry. Furthermore, it is not possible to go from the plane to a torus via a conformal transformation as the genus of the geometries differ.
The internal modes of the spherical and planar BTZ black holes are similar because the metrics are similar. We have two well behaving modes inside the black hole and one outside. Thus there is nothing stopping the construction of the phases, as we did for the planar BTZ black hole. We will check whether other black holes permit a similar construction.

5.2 Power series method

Finding a Explicit solution of a differential equation can be difficult. Therefore it often easier to construct a series that converges to the solution [9].

$$y(x) = \sum_{n=0}^{\infty} a_n x^{n+r} \tag{238}$$

is a power series. Substituting this series in a differential equation will lead to constraints on a_n and r, we require that $a_0 \neq 0$ otherwise this would lead to a redefinition of r. On all ordinary points this construction leads to a solution of the equation. Furthermore using the identity theorem for holomorphic functions this series can often be identified with an explicit form. A series can be constructed around every point x_0, it is often easier to shift the variable such that we work around the point $x' = x - x_0 = 0$. For simplicity we have assumed that such a shift has taken place where necessary. So far we talked about ordinary points, however, singularities are often physically relevant therefore a treatment of those points is needed. Although this discussion can be expended to higher order equations, limit ourself to second order differential equations, as they are the most relevant for us. Consider the following general form of a second order homogeneous ordinary linear differential equation.

$$y'' + P(x)y' + Q(x)y = 0 \tag{239}$$

We can classify our points as follows:

- x_1 is a ordinary point when both $P(x_1)$ and $Q(x_1)$ are regular (non-singular)
- x_2 is a regular singular point when both $(x - x_2)P(x_2)$ and $(x - x_2)^2Q(x_2)$ are regular
- x_3 is a essential (or irregular) singular point when both $(x - x_3)P(x_3)$ and $(x - x_3)^2Q(x_3)$ are irregular (singular)

When we substitute (238) in (239) and at the lowest power of x this must vanish in order for the series to be a solution as it is the leading order term near zero. This places a constrained on r, this is called the indicial equation. The solutions of the indicial equation are called exponents. In the case of a ordinary point this simple. Because both $P(x)$ and $Q(x)$ are regular they can be expanded using a Taylor series.

$$P(x) = \sum_{n=0}^{\infty} p_n x^n \qquad\qquad Q(x) = \sum_{n=0}^{\infty} q_n x^n \tag{240}$$

We clearly see that the lowest power of x will come from y''. Therefore the leading order near zero is $r(r-1)x^{r-2}$. Thus the indicial equation is $r(r-1) = 0$. For an ordinary point the two solutions of the indicial equation are guaranteed two give two independent solutions. For a regular singular point, we again expand $P(x)$ and $Q(x)$, however, because they are singular we need a Laurent series instead of a Taylor series. We know that $P(x)$ has a pole of at most order one and $Q(x)$ has a pole of at most order two, therefore they can be expanded in the following series.

$$P(x) = \sum_{n=-1}^{\infty} p_n x^n \qquad\qquad Q(x) = \sum_{n=-2}^{\infty} q_n x^n \tag{241}$$

This time there will be some more contributions to the indicial equation.

$$r(r-1) + p_{-1}r + q_{-2} = 0 \tag{242}$$

This time we are not guaranteed two solutions. By Fuchs' theorem we obtain two independent series solutions when the two exponents r_1, r_2 have the following relation $r_1 - r_2 \neq n \forall n \in \mathbb{N}$ holds. If $r_1 - r_2 = n$

for some $n \in \mathbb{N}$ we must replace the second (the lowest of the two exponents) series solution with the following:

$$y_2 = y_1 \log(x) + \sum_{n=0}^{\infty} b_n x^{n+r_2} \tag{243}$$

where $b_0 \neq 0$ and y_1 is the power series solution obtained with exponent r_1. In both the cases of the ordinary point and the regular singular point we are guaranteed convergence of our solution as long the expansions of P and Q hold. Therefore the radius of converges is the distance to the next singular point. We should be a bit careful with regular singular point itself as at that point convergence is not guaranteed. In the case of essential singularity this method does not necessarily work and if a series is obtained convergence must be proven independently.

5.3 Rindler modes power series

We already discussed the Rindler modes in great detail, however, we will develop the modes again using the power series method. Moreover we are not interested in the entire power series only the leading terms. Therefore the indicial equation has all the information we need. The equation for the Rindler modes has already been given in equation (27).

$$\rho^2 f_\omega'' + \rho f_\omega' - (\rho^2 m^2 - \omega^2) f_\omega = 0 \tag{244}$$

We construct the power series around $\rho = 0$ therefore we approximate $f \approx \rho^c$ and collect the leading order terms. The indicial equation is in this case:

$$c^2 = -\omega^2 \tag{245}$$

Also investigation of the singular point $\rho = 0$ reveals that is an regular singular point. Therefore we are guaranteed to obtain two independent power series. We will compare the leading orders of the modes around black holes to this result.

5.4 BTZ modes power series

Although the BTZ black hole has been studied in section 4 it is good to check the results we already have obtained. Furthermore we try to find a intuitive reason for the behaviour of the modes in relation to the dimension of the space. We have already done some steps. We started with the BTZ metric (129) and obtained the wave equation (184) from the Klein-Gordon equation in a curved space-time (26). For reader convenience we restate the obtained wave equation.

$$\left(\frac{\omega^2}{r^2 - r_0^2} - \frac{k^2}{r^2} - m^2\right) f_{\omega,k}(r) + \left(3r - \frac{r_0^2}{r}\right) f_{\omega,k}'(r) + \left(r^2 - r_0^2\right) f_{\omega,k}''(r) = 0 \tag{246}$$

We want obtain a power series around the point $r = 0$, therefore we calculate the indicial equation. We make the approximation $f \approx r^c$ and focus on the leading order terms.

$$c^2 + \frac{k^2}{r_0^2} = 0 \tag{247}$$

Therefore we see that the leading orders of the modes go as $c_\pm = \pm i \frac{k}{r_0}$. Looking back at the modes obtained (185), (186), we indeed see that the modes have their leading order going as $r^{\pm 2a}$.
To compare to the Rindler case we need to obtain a power series around the horizon. Therefore we repeat the last steps, this time with $f \approx \epsilon^c$ with $\epsilon = r - r_0$. Here the indicial equation is:

$$c^2 = -\frac{\omega^2}{(2r_0)^2} \tag{248}$$

Which is similar to the Rindler case except for a scale difference. In both cases $r = 0, r = r_0$ the singular points are regular singular points.

5.5 Schwarzschild black hole

We repeat the discussion of the BTZ modes near the singularity and near the horizon. We now use the Schwarzschild metric as the background.

$$ds^2 = -\left(1 - \frac{r_0}{r}\right) dt^2 + \left(1 - \frac{r_0}{r}\right)^{-1} dr^2 + r^2 d\Omega^2 \tag{249}$$

$$d\Omega^2 = d\theta^2 + \sin(\theta)^2 d\phi^2 \tag{250}$$

The Klein-Gordon equation (26) then becomes, where we have used $\sqrt{-g} = r^2 \sin(\theta)$:

$$\left(\frac{-1}{1 - r_0/r}\frac{\partial^2}{\partial t^2} + \frac{1}{r^2}\frac{\partial}{\partial r}(1 - r_0/r)r^2\frac{\partial}{\partial r} + \frac{1}{r^2}\left(\frac{1}{\sin(\theta)}\frac{\partial}{\partial \theta}\sin(\theta)\frac{\partial}{\partial \theta} + \frac{1}{\sin(\theta)^2}\frac{\partial^2}{\partial \phi^2}\right) - m^2\right)\psi = 0 \tag{251}$$

Because of the symmetries of this equation we can use following ansatz:

$$\psi_{\omega,l,m}(t, r, \theta, \phi) = e^{-\omega t} Y^l_m(\theta, \phi) f_{\omega,l,m}(r) \tag{252}$$

where $Y^l_m(\theta, \phi)$ are the spherical harmonics. then $f_{\omega,l,m}(r)$ must satisfy then following equation.

$$\left(\frac{\omega^2}{1 - r_0/r} - m^2 + \frac{l(l+1)}{r^2} + \frac{1}{r^2}\frac{\partial}{\partial r}(1 - r_0/r)r^2\frac{\partial}{\partial r}\right) f_{\omega,l,m}(r) = 0 \tag{253}$$

We again want obtain a power series around the point $r = 0$, therefore we calculate the indicial equation. We make the approximation $f \approx r^c$ and focus on the leading order terms.

$$\omega^2 r^{c+1} + l(l+1)r^{c-2} - r_0 c^2 r^{c-3} + c(c+1)r^{c-2} - m^2 r^c = 0 \tag{254}$$

therefore the indicial equation is $c^2 = 0$. We notice that the behave of the leading orders of these modes are very different from the BTZ black hole. Therefore results obtained near $r = 0$ may be very different for both cases . Near the horizon we expand near $\epsilon = r - r_0 = 0$ and obtain as our indicial equation

$$c^2 = -\omega^2 r_0^2 \tag{255}$$

Again similar as the Rindler and BTZ cases.

5.6 Higher dimension Schwarzschild black holes

To whether there is some structure in the behaviour of the modes depending on the dimension of the space. Therefore we look at the higher dimension $(N + 1)$ Schwarzschild metric.

$$ds^2 = -\left(1 - \frac{C}{r^{N-2}}\right) dt^2 + \left(1 - \frac{C}{r^{N-2}}\right)^{-1} dr^2 + r^2 d\Omega^2_{N-1} \tag{256}$$

again we obtain the wave equation from the Klein-Gordon equation together with an ansatz similar to the ansatz in the case of the normal Schwarzschild metric. Here we have that $\sqrt{-g} \propto r^{N-1}$, furthermore we assume that their is an higher dimension ansatz similar to the spherical harmonics with eigenvalue L.

$$\left(\frac{\omega^2}{1 - C/r^{N-2}} - m^2 + \frac{L}{r^2} + \frac{1}{r^{N-1}}\frac{\partial}{\partial r}(1 - C/r^{N-2})r^{N-1}\frac{\partial}{\partial r}\right) f_{\omega,l,m}(r) = 0 \tag{257}$$

We again want obtain a power series around the point $r = 0$, therefore we calculate the indicial equation. We make the approximation $f \approx r^c$ and focus on the leading order terms.

$$\omega^2 r^{c+N-2} + Lr^{c-2} - Cc^2 r^{c-N} + c(c + N - 2)r^{c-2} - m^2 r^c = 0 \tag{258}$$

therefore the indicial equation is $c^2 = 0$ for $N > 2$. This leads to the same behaviour for all $N > 2$. The black hole disappears for $N = 2$ and is therefore not that interesting. Near the horizon we obtain for $N > 2$:

$$c^2 = -\frac{\omega^2 r_0^2}{(N-2)^2} \tag{259}$$

Where $r_0^{N-2} = C$. Again similar to the previous cases. Therefore near the horizon we expect the same behaviour as in our Rindler and BTZ discussion.

5.7 AdS-Schwarzschild black holes

By adding a factor of r^2 to the term that govern the shape of the black hole the black hole becomes asymptomatically AdS.

$$ds^2 = -\left(r^2 + 1 - \frac{C}{r^{N-2}}\right) dt^2 + \left(r^2 + 1 - \frac{C}{r^{N-2}}\right)^{-1} dr^2 + r^2 d\Omega_{N-1}^2 \tag{260}$$

For large r we obtain:

$$ds^2 = -r^2 dt^2 + r^{-2} dr^2 + r^2 d\Omega_{N-1}^2 \tag{261}$$

Which is, after putting $r = 1/z$, the AdS metric. Therefore these black holes can also be studied in the framework of AdS/CFT. As we are only looking for the lowest power of r, the addition will not affect the indicial equation. The behaviour near the singularity or near the horizon of the modes is the same as for the normal Schwarzschild black hole.
All the black holes we have encountered so far have the same behaviour as our in detail treated cases, together with the fact that close to the horizon the space looks like Rindler space, we expect that the same conclusions hold as for the perturb Hartle-Hawking state.

5.8 Interacting particles

The full discussion about interacting fields is beyond the scope of this thesis. However, as said in section 4.10, a particle with energy E_b at the boundary released at $t = t_w$ will have a proper energy of:

$$E_p \sim \frac{E_b}{r_0} e^{r_0 t_w} \tag{262}$$

Which, if dropped early enough, can be arbitrary high. the proper energy can even be of the Planck scale or beyond that. Therefore anything that would encounter this particle would not survive the encounter. Thus a particle dropped early in the left universe would act as a firewall for particles entering the black hole from the right universe. However this is not inherent to the black hole and, therefore, we argue that to resolve the information paradox one can not relay on such an argument.

5.9 Actual black hole

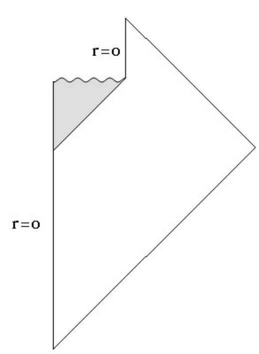

Figure 8: Penrose diagram of an black hole formed by a collapsing star. The grey area corresponds to the inside of the black hole.

In the end we want to fully understand a black hole formed by a collapse star on the background of the current cosmological models. Such a black hole has some vastly different properties then the ones we have treated so far. The Penrose diagram has no 'left' universe, see figure 8. Therefore we lack a clear interpretation of the the thermofield double. The black hole is not time-independent as it evaporates. Moreover, the black hole is not eternal.
All of these things are different from the black holes we have studied. However, if a thermofield double can be constructed for such a black hole then phase changes to that state will leave the outside world unchanged. Thus our discussion is still relevant for that case.

6 Conclusions

We have studied a free scalar field on a curved background. First in the case of Rindler space, which closely resembles the near horizon patch of a black hole. We have seen that to describe the entire system we need use an entangled state as ground state. Moreover we can smoothly crossover the boundaries, Rindler horizons, and construct the future wedge through analytic continuation. Moreover the left and right wedges are filled with particles in a thermal ensemble. From this ensemble the black hole temperature is derived.
We generalized this entangled state by allowing phase changes. This did not affect physics within either the left or right wedge. The future wedge and the relation between left and right was affected. In those cases both the two-point function and the geodesic distance were changed. Moreover, the phase changes can be reinterpreted as various time shifts.
We repeated the discussion for the planar BTZ black hole and obtained similar results. We obtained the quantum state of the black hole, the Hartle-Hawking state. And constructed the inside through analytic continuation from the two outside universes. Perturbations to the Hartle-Hawking state, in the form of phase changes, did not affect the outside. In this case the changed phases can be reinterpreted as how one analytically continues from one CFT to the other.
Modes of other black holes show similar behaviour around the horizon. We expect that our construction is also possible in these cases, because our construction and reinterpretation of changed phases in the Hartle-Hawking state only relied on the modes and on how time evolution interacted with these modes.
It would be fine tuning to, a priori, set all the phases in the Hartle-Hawking state to zero, because from a observer outside the black hole no effect is seen from these phases. However, the effect of these changed phases should be taken into account as the geodesic distance is used to probe the interior of the black hole [8]. Furthermore, we have seen no indication of a firewall on the horizon. We have been able to construct the inside of the black hole from the two outside regions, and from the boundary CFT's in the case of the BTZ black hole.
Although no local physics outside the black hole is affected by the changed phases, non-local effects are changed. It has been proposed that small non-local effects can restore unitairity [10] and that is affected by the changed phases. How and whether these phases correspond to black hole micro-states is a question that could be explored in further detail. Also how our construction applies to a time dependant or one sided black hole is unclear. We hope to revisit these questions in future works.

7 Acknowledgements

The author would like to thank Kyriakos Papadodimas for his helpful discussions, which has shaped much of this work.

8 References

[1] S. D. Mathur, *The information paradox: A pedagogical introduction.* arXiv:hep-th/09091038v2 2011

[2] S. D. Mathur, *What is the dual of two entangled CFTs?* arXiv:hep-th/14026378v1 2014

[3] A. Almheiri, D. Marolf, J. Polchinski, J. Sully, *Black Holes: Complementarity or Firewalls?* arXiv:hep-th/12073123v4 2013

[4] J. Maldacena, *Eternal black holes in Anti-de-Sitter*. arXiv:hep-th/0106112v6 2001

[5] N. D. Birrell, P. C. W. Davies, *Quantum Fields in Curved Space* Cambridge: Cambride university press 1982

[6] W. Israel *Thermo Field Dynamics Of Black Holes*. Phys. Lett. A 57 p107-110, 1976

[7] W. Miller *Symmetry groups and their applications*. New York: Academic press 1973

[8] S. H. Shenker, D. Stanford, *Black holes and the butterfly effect*. arXiv:hep-th/13060622v3 2014

[9] G. B. Arfken, H. J. Weber, F. E. Harris, *Mathematical Methods for Physicists*. 7th edition New York: Academic press 2013

[10] K. Papadodimas, S. Raju, *An Infalling Observer in AdS/CFT*. arXiv:hep-th/1211.6767v2 2013

A Small proofs

A.1 Periodic euclidean fields and finite temperature fields

To obtain quantum mechanical function in a thermal ensemble, the most strait forward approach is from analytic continuation from a Euclidean function with periodic time. So we identify $\tau_E = \tau_E + \beta$, where β is period of the Euclidean time. We look at the two-point function where we return to the same point after one period. So $x' = x$, we then obtain:

$$\left\langle x', \tau_E' \right| x, \tau_E \rangle = \left\langle x', 0 \right| e^{-iH(\tau_E - \tau_E')} \left| x, 0 \right\rangle \tag{263}$$

$$= \sum_{m,n} \left\langle x', 0 \right| n \rangle \left\langle n \right| e^{-iH(\tau_E - \tau_E')} \left| m \right\rangle \left\langle m \right| x, 0 \rangle \tag{264}$$

$$= \sum_{n} \psi_n \psi_n^\dagger e^{-iE_n(\tau_E - \tau_E')} \tag{265}$$

We Wick rotate to real time $t = -i\tau_E$ and return to the same point after one period $\tau_E' = \tau_E + \beta$.

$$\left\langle x', t' \right| x, t \rangle = \sum_n \psi_n \psi_n^\dagger e^{-iE_n(t-t')} \tag{266}$$

$$= \sum_n \psi_n \psi_n^\dagger e^{-\beta E_n} \tag{267}$$

$$= \mathrm{Tr}\left(e^{-\beta H}\right) \tag{268}$$

Which is the partition function of a field with inverse temperature β. Therefore calculation in a field with euclidean signature and period β and a field with temperature $T = 1/\beta$ are equivalent.

A.2 Relation between geodesic distance and the two point function

We can interpret the following two point function as a path integral from y to x.

$$\langle \hat{\phi}(x)\hat{\phi}(y)\rangle \sum_{allpaths} e^{iS} \tag{269}$$

For very heavy particle the classical path dominates the path integral.

$$\langle \hat{\phi}(x)\hat{\phi}(y)\rangle \sim e^{iS} \tag{270}$$

$$\langle \hat{\phi}(x)\hat{\phi}(y)\rangle \sim e^{-S_E} \tag{271}$$

Where S_E is the Euclidean action over the appropriate Lagrangian, which is:

$$\mathcal{L} = a\sqrt{g_{\mu\nu}\dot{x}^\mu \dot{x}^\nu} \tag{272}$$

Where a is still free. In the non-relativistic limit this becomes:

$$\mathcal{L} \approx a\sqrt{1-v^2} \approx a\left(1 - \frac{1}{2}v^2\right) \tag{273}$$

Thus to obtain the classical kinetic energy term we need to identify $a = m$. The geodesic distance d is given by:

$$d(x,y) = \int \sqrt{g_{\mu\nu}\dot{x}^\mu \dot{x}^\nu} ds \tag{274}$$

Where x and y are the endpoints. Using this in equation (271) we obtain:

$$\langle \hat{\phi}(x)\hat{\phi}(y)\rangle \sim e^{-md(x,y)} \tag{275}$$

Thus the two point function is related to the geodesic distance. Furthermore, the classical path will dominate more as the particle becomes heavier. Thus this equation becomes more precise as the mass increases.

$$\langle\hat{\phi}(x)\hat{\phi}(y)\rangle \sim e^{-md(x,y)} \tag{276}$$

$$\langle\hat{\phi}(x)\hat{\phi}(y)\rangle \sim e^{-md(x,y)} \tag{277}$$

where $d(x,y)$ is geodesic distance.

A.3 Passing through the number operator

We know that time evolution is governed by (up to a overall phase):

$$\hat{U}(t) = e^{-i\omega\hat{N}t} \tag{278}$$
$$\hat{N} = \hat{a}^\dagger\hat{a} \tag{279}$$
$$\hat{\phi}(t) = \hat{U}^{-1}(t)\hat{\phi}(0)\hat{U}(t) \tag{280}$$

We need to know how this exponent of the number operator $\hat{N}$ interacts with creation and annihilation operators. For example:

$$e^{c\hat{N}}\hat{a}\,|n\rangle = \sqrt{n}e^{c\hat{N}}\,|n-1\rangle \tag{281}$$
$$= \sqrt{n}e^{c(n-1)}\,|n-1\rangle \tag{282}$$
$$= \hat{a}e^{c(n-1)}\,|n\rangle \tag{283}$$
$$= \hat{a}e^{c(\hat{N}-1)}\,|n\rangle \tag{284}$$

Which can be easily generelized to higher powers of $\hat{N}$.

$$e^{c\hat{N}^m}\hat{a}\,|n\rangle = \sqrt{n}e^{c\hat{N}^m}\,|n-1\rangle \tag{285}$$
$$= \sqrt{n}e^{c(n-1)^m}\,|n-1\rangle \tag{286}$$
$$= \hat{a}e^{c(n-1)^m}\,|n\rangle \tag{287}$$
$$= \hat{a}e^{c(\hat{N}-1)^m}\,|n\rangle \tag{288}$$

A.4 Calculation of series

let

$$S = 1 + x + x^2 + x^3 \dots \tag{289}$$

then

$$1 + xS = 1 + x + x^2 + x^3 \dots = S \tag{290}$$

thus

$$S = \frac{1}{1-x} \tag{291}$$

There is a singularity at $x = 1$ therefore this does not hold at that point. It can be analytically continued beyond that point. So

$$\frac{1}{1-x} = 1 + x + x^2 + x^3 \dots \tag{292}$$

Furthermore let

$$\hat{S} = x + 2x^2 + 3x^3 + \dots \tag{293}$$

which can be rewritten as

$$\hat{S} = x\frac{d}{dx}x + x\frac{d}{dx}x^2 + x\frac{d}{dx}x^3 + \dots \tag{294}$$

$$= x\frac{d}{dx}(1 + x + x^2 + x^3 + \dots) \tag{295}$$

$$= x\frac{d}{dx}\frac{1}{1-x} \tag{296}$$

$$= \frac{x}{(1-x)^2} \tag{297}$$

Again there is a singularity at $x = 1$. The same method can be used in similar cases.